17-[[(2-dimethylamino)ethyl]amino]geldanamycin (17DMAG, NSC 707545) in C.B-17 SCID mice bearing MDA-MB-231 human breast cancer xenografts. Cancer Chemother Pharmacol. 2005; 55(1):21-32.

21. Koizumi H, Yamada T, Takeuchi S, Nakagawa T, Kita K, Nakamura T, et al. Hsp90 inhibition overcomes HGF-triggering resistance to EGFR-TKIs in EGFR-mutant lung cancer by decreasing client protein expression and angiogenesis. Journal of thoracic oncology. 2012; 7(7):1078-1085.
22. Birchmeier C, Birchmeier W, Gherardi E, Vande Woude GF. Met, metastasis, motility and more. Nature reviews. Molecular cell biology. 2003; 4(12):915-925.
23. Yano S, Wang W, Li Q, Matsumoto K, Sakurama H, Nakamura T, Ogino H, Kakiuchi S, Hanibuchi M, Nishioka Y, Uehara H, Mitsudomi T, Yatabe Y, et al. Hepatocyte growth factor induces gefitinib resistance of lung adenocarcinoma with epidermal growth factor receptor-activating mutations. Cancer research. 2008; 68(22):9479-9487.
24. Yano S, Yamada T, Takeuchi S, Tachibana K, Minami Y, Yatabe Y, et al. Hepatocyte growth factor expression in EGFR mutant lung cancer with intrinsic and acquired resistance to tyrosine kinase inhibitors in a Japanese cohort. Journal of thoracic oncology. 2011; 6(12):2011-2017.
25. Masuya D, Huang C, Liu D, Nakashima T, Kameyama K, Haba R, Ueno M, Yokomise H, et al. The tumour-stromal interaction between intratumoral c-Met and stromal hepatocyte growth factor associated with tumour growth and prognosis in non-small-cell lung cancer patients. British journal of cancer. 2004; 90(8):1555-1562.
26. Meert AP, Martin B, Delmotte P, Berghmans T, Lafitte JJ, Mascaux C, et al. The role of EGF-R expression on patient survival in lung cancer: a systematic review with meta-analysis. The European respiratory journal. 2002; 20(4):975-981.
27. Engelman JA, Zejnullahu K, Mitsudomi T, Song Y, Hyland C, Park JO, et al. MET amplification leads to gefitinib resistance in lung cancer by activating ERBB3 signaling. Science. 2007; 316(5827):1039-1043.
28. Zhang Z, Lee JC, Lin L, Olivas V, Au V, LaFramboise T, et al. Activation of the AXL kinase causes resistance to EGFR-targeted therapy in lung cancer. Nat genetics. 2012; 44(8):852-860.
29. Takezawa K, Pirazzoli V, Arcila ME, Nebhan CA, Song X, de Stanchina E, et al. HER2 Amplification: A Potential Mechanism of Acquired Resistance to EGFR Inhibition in EGFR-Mutant Lung Cancers That Lack the Second-Site EGFRT790M Mutation. Cancer discovery. 2012; 2(10):922-933.
30. Straussman R, Morikawa T, Shee K, Barzily-Rokni M, Qian ZR, Du J, et al. Tumour micro-environment elicits innate resistance to RAF inhibitors through HGF secretion. Nature. 2012; 487(7408):500-504.
31. Hilmi C, Larribere L, Giuliano S, Bille K, Ortonne JP, Ballotti R, et al. IGF1 promotes resistance to apoptosis in melanoma cells through an increased expression of BCL2, BCL-X(L), and survivin. J Invest Dermatol. 2008; 128(6):1499-1505.
32. Takezawa K, Okamoto I, Nishio K, Janne PA, Nakagawa K. Role of ERK-BIM and STAT3-survivin signaling pathways in ALK inhibitor-induced apoptosis in EML4-ALK-positive lung cancer. Clinical cancer research. 2011; 17(8):2140-2148.
33. Natan S, Tsarfaty G, Horev J, Haklai R, Kloog Y, Tsarfaty I, et al. Interplay between HGF/SF-Met-Ras signaling, tumor metabolism and blood flow as a potential target for breast cancer therapy. Oncoscience. 2014; 1: 30-38.
34 Tang C, Fontes Jardim DL, Falchook GS, Hess K, Fu S, Wheler JJ, et al. MET nucleotide variations and amplification in advanced ovarian cancer: characteristics and outcomes with c-Met inhibitors. Oncoscience. 2014; 11: 5-13.
35. Janku F. Tumor heterogeneity in the clinic: is it a real problem?. Therapeutic advances in medical oncology. 2014; 6(2):43-51.
36. Socinski MA, Goldman J, El-Hariry I, Koczywas M, Vukovic V, Horn L, Paschold E,Salgia R, West H, Sequist L.V, Bonomi P, Brahmer J, Chen L.C, et al. A multicenter phase II study of ganetespib monotherapy in patients with genotypically defined advanced non-small cell lung cancer. Clinical cancer research. 2013; 19(11):3068-3077.
37. Koivunen JP, Mermel C, Zejnullahu K, Murphy C, Lifshits E, Holmes AJ, et al. EML4-ALK fusion gene and efficacy of an ALK kinase inhibitor in lung cancer. Clinical cancer research. 2008; 14(13):4275-4283.
38. Montesano R, Matsumoto K, Nakamura T, Orci L. Identification of a fibroblast-derived epithelial morphogen as hepatocyte growth factor. Cell. 1991; 67(5):901-908.
39. Yasumoto K, Yamada T, Kawashima A, Wang W, Li Q, Donev IS, et al. The EGFR ligands amphiregulin and heparin-binding egf-like growth factor promote peritoneal carcinomatosis in CXCR4-expressing gastric cancer. Clinical cancer research. 2011; 17(11):3619-3630.
40. Ueki T, Kaneda Y, Tsutsui H, Nakanishi K, Sawa Y, Morishita R, Matsumoto K, Nakamura T, Takahashi H, Okamoto E, Fujimoto J, et al. Hepatocyte growth factor gene therapy of liver cirrhosis in rats. Nature medicine. 1999; 5(2):226-230.

OPEN

Triple Inhibition of EGFR, Met, and VEGF Suppresses Regrowth of HGF-Triggered, Erlotinib-Resistant Lung Cancer Harboring an *EGFR* Mutation

Junya Nakade, MS, Shinji Takeuchi, MD, PhD,* Takayuki Nakagawa, MS,* Daisuke Ishikawa, MD,* Takako Sano, PhD,* Shigeki Nanjo, MD,* Tadaaki Yamada, MD, PhD,* Hiromichi Ebi, MD, PhD,* Lu Zhao, MS,* Kazuo Yasumoto, MD, PhD,* Kunio Matsumoto, PhD,† Kazuhiko Yonekura, PhD,‡ and Seiji Yano, MD, PhD**

Introduction: Met activation by gene amplification and its ligand, hepatocyte growth factor (HGF), imparts resistance to epidermal growth factor receptor (EGFR) tyrosine kinase inhibitors (TKIs) in *EGFR*-mutant lung cancer. We recently reported that Met activation by HGF stimulates the production of vascular endothelial growth factor (VEGF) and facilitates angiogenesis, which indicates that HGF induces EGFR-TKI resistance and angiogenesis. This study aimed to determine the effect of triple inhibition of EGFR, Met, and angiogenesis on HGF-triggered EGFR-TKI resistance in *EGFR*-mutant lung cancer.

Methods: Three clinically approved drugs, erlotinib (an EGFR inhibitor), crizotinib (an inhibitor of anaplastic lymphoma kinase and Met), and bevacizumab (anti-VEGF antibody), and TAS-115, a novel dual TKI for Met and VEGF receptor 2, were used in this study. *EGFR*-mutant lung cancer cell lines PC-9, HCC827, and *HGF*-gene–transfected PC-9 (PC-9/HGF) cells were examined.

Results: Crizotinib and TAS-115 inhibited Met phosphorylation and reversed erlotinib resistance and VEGF production triggered by HGF in PC-9 and HCC827 cells in vitro. Bevacizumab and TAS-115 inhibited angiogenesis in PC-9/HGF tumors in vivo. Moreover, the triplet erlotinib, crizotinib, and bevacizumab, or the doublet erlotinib and TAS-115 successfully inhibited PC-9/HGF tumor growth and delayed tumor regrowth associated with sustained tumor vasculature inhibition even after cessation of the treatment.

Conclusion: These results suggest that triple inhibition of EGFR, HGF/Met, and VEGF/VEGF receptor 2, by either a triplet of clinical drugs or TAS-115 combined with erlotinib, may be useful for controlling progression of *EGFR*-mutant lung cancer by reversing EGFR-TKI resistance and for inhibiting angiogenesis.

Divisions of *Medical Oncology and †Tumor Dynamics and Regulation, Cancer Research Institute, Kanazawa University, Kanazawa, Japan; and ‡Tsukuba Research Center, Taiho Pharmaceutical Co., Ltd., Tsukuba, Japan.

Disclosure: Dr. Yano received honoraria from Chugai Pharma and AstraZeneca and research funding from Chugai Pharma. Mr. Nakagawa is an employee of Eisai Co., Ltd. Dr. Yonekura is an employee of Taiho Pharmaceutical Co., Ltd. The remaining authors declare no conflict of interest.

Address for correspondence: Seiji Yano, MD, PhD, Division of Medical Oncology, Cancer Research Institute, Kanazawa University, 13-1 Takara-machi, Kanazawa, Ishikawa 920–0934, Japan. E-mail: syano@staff.kanazawa-u.ac.jp

ISSN: 1556-0864/14/0906-0775

Key Words: Hepatocyte growth factor, Vascular endothelial growth factor, Epidermal growth factor receptor-tyrosine kinase inhibitor resistance, Lung cancer, Epidermal growth factor receptor mutation.

(*J Thorac Oncol.* 2014;9: 775–783)

Lung cancer is the leading cause of cancer-related deaths worldwide. Recent advances in molecular biology have identified driver oncogenes such as epidermal growth factor receptor (EGFR) mutations or the echinoderm microtubule–associated protein-like 4/anaplastic lymphoma kinase (ALK) fusion gene in non–small-cell lung cancer (NSCLC). In the treatment of NSCLCs harboring these driver oncogenes, the use of EGFR tyrosine kinase inhibitors (TKIs; such as gefitinib and erlotinib) and an ALK inhibitor (such as crizotinib) to block driver oncogene survival signals resulted in marked tumor regression.[1–4] Despite these clinical successes, tumors acquire resistance to those agents in almost all cases during the course of therapy.[5]

Recently, several mechanisms of EGFR-TKI resistance have been identified and classified as follows: (1) alteration of the target *EGFR* gene (e.g., T790M gatekeeper mutation)[6,7]; (2) activation of bypass resistance signals (e.g., *Met* gene amplification,[8] hepatocyte growth factor [HGF] overexpression,[9] and activation of the nuclear factor-kappa B (NFkB) pathway[10] and Gas6-AXL axis)[11]; and (3) other mechanisms such as transformation to small-cell lung cancer,[12–14] epithelial-to-mesenchymal transition,[15–17] alteration of microRNA,[18] and down-regulation of MED12.[19] Previously, we demonstrated that HGF activates, through the Met/PI3K/Akt pathway, bypass signals that trigger resistance; overexpression of HGF was observed more frequently than T790M and *Met* amplification in tumors from patients with NSCLC who acquired EGFR-TKI resistance in a Japanese cohort.[20] These findings indicate that HGF is a clinically relevant target for overcoming EGFR-TKI resistance in *EGFR*-mutant lung cancer.

Angiogenesis is essential for the progression of various types of solid tumors, including NSCLC. Vascular endothelial growth factor (VEGF) is the most prominent proangiogenic molecule and is considered to be a therapeutic target in NSCLC. We previously reported that overexpressed HGF

stimulates VEGF production by means of phosphorylation of Met/Gab1 and promotes tumor growth by stimulating angiogenesis in *EGFR*-mutant lung cancer models,[21] which indicates that HGF is a critical inducer of not only EGFR-TKI resistance but also angiogenesis in *EGFR*-mutant lung cancer. Therefore, we hypothesized that triple inhibition of the driver signal (EGFR), bypass resistance signal (Met), and angiogenesis (VEGF) may be beneficial for controlling the progression of *EGFR*-mutant lung cancer with HGF-triggered EGFR-TKI resistance.

EGFR-TKIs, erlotinib, gefitinib, ALK-TKI, crizotinib, and the anti-VEGF antibody bevacizumab have been clinically approved as molecularly targeted drugs in many countries. Crizotinib is known to have activity against Met in addition to ALK and c-ros oncogene 1, receptor tyrosine kinase (ROS1).[22,23] In the present study, we investigated the therapeutic effect of triple inhibition against HGF-triggered, EGFR-TKI–resistant lung cancer harboring an *EGFR* mutation by using clinically available targeted drugs, namely, erlotinib, crizotinib, and bevacizumab. We further assessed the therapeutic potential of erlotinib and TAS-115 (Supplementary Figure 1, Supplementary Digital Content 1, http://links.lww.com/JTO/A570), a novel VEGF receptor 2 (VEGFR-2) inhibitor, which can be orally administered and has Met inhibitory activity, and we compared this doublet treatment with the clinically available triplet. In this study, we demonstrate that the doublet inhibited the progression of HGF-overexpressing *EGFR*-mutant lung cancer more efficiently than the clinically available triplet treatment. Moreover, TAS-115 combined with erlotinib also controlled tumor growth well and, remarkably, delayed regrowth even after cessation of the treatment.

MATERIALS AND METHODS

Cell Cultures and Reagents

The *EGFR*-mutant human lung adenocarcinoma cell lines PC-9 (del E746_A750) and HCC827, with deletions in *EGFR* exon 19, were purchased from Immuno-Biological Laboratories Co. (Gunma, Japan) and from American Type Culture Collection (Manassas, VA) respectively.[21] Human *HGF*-gene transfectant (PC-9/HGF) and vector control (PC-9/Vec) cells were established as previously described.[24] These cell lines were maintained in RPMI-1640 medium supplemented with 10% fetal bovine serum (FBS) and antibiotics. All cells were passaged for less than 3 months before renewal from frozen, early-passage stocks. The human embryonic lung fibroblast cell line MRC-5 was purchased from the Health Science Research Resources Bank (Osaka, Japan). MRC-5 (P30–35) cells were maintained in Dulbecco's modified Eagle's medium with 10% FBS, 100 units/ml penicillin, and 100 μg/ml streptomycin. Human dermal microvascular endothelial cells (HMVECs) were incubated in RPMI-1640 medium with 10% FBS (control), RPMI-1640 medium with 10% FBS plus VEGF, or HuMedia-MvG with different concentrations of TAS-115 for 72 hours. Thereafter, cell viability was determined by thiazolyl blue tetrazolium bromide (MTT) assay. Cells were regularly screened for mycoplasma by using MycoAlert Mycoplasma Detection Kits (Lonza, Rockland, ME). The cell lines were authenticated at the laboratory of the National Institute of Biomedical Innovation (Osaka, Japan) by short tandem repeat analysis. TAS-115 was synthesized by Taiho Co., Ltd (Tokyo, Japan). Erlotinib and crizotinib were obtained from Selleck Chemicals (Houston, TX). Bevacizumab was obtained from Chugai Pharma (Tokyo, Japan). Human recombinant HGF was prepared as previously described.[24]

Production of HGF and VEGF in Cell Culture Supernatants

Cells (2×10^5) were cultured in a 2 ml of culture medium with 10% FBS for 24 hours, washed with phosphate-buffered saline (PBS), and incubated for 48 hours in the medium supplemented with 10% FBS. In some experiments, HGF was added to the medium. The culture media was harvested and centrifuged, and the supernatants were stored at −80°C until analysis. The concentrations of HGF and VEGF were determined by IMMUNIS HGF EIA (Institute of Immunology, Tokyo, Japan) or Quantikine VEGF enzyme-linked immunosorbent assay (R&D Systems, Minneapolis, MN), respectively, according to the respective manufacturer's protocol. All samples were run in duplicate. Color intensity was measured at 450 nm by using a spectrophotometric plate reader. Growth factor concentrations were determined by comparison with standard curves. The detection limits for HGF and VEGF were 100 and 31 pg/ml, respectively.

Cell Viability Assay

Cell growth was measured using the MTT dye reduction method.[24] Tumor cells were plated into 96-well plates at a density of 2×10^3 cells/100 ml RPMI-1640 medium with 10% FBS per well. After 24-hour incubation, various reagents were added to each well, and the cells incubated for a further 72 hours, followed by the addition of 50 μl of MTT solution (2 mg/ml; Sigma, St. Louis, MO) to each well and incubation for 2 hours. The media containing MTT solution was removed, and the dark blue crystals were dissolved by adding 100 ml of dimethyl sulfoxide. The absorbance of each well was measured with a microplate reader at test and reference wavelengths of 550 and 630 nm, respectively. The percentage of growth is shown relative to untreated controls. Each reagent concentration was tested at least in triplicate during each experiment, and each experiment was conducted at least three times.

Antibodies and Western Blotting

Protein aliquots of 25 μg each were resolved by sodium dodecyl sulfate-polyacrylamide gel (Bio-Rad, Hercules, CA) electrophoresis and transferred to polyvinylidene difluoride membranes (Bio-Rad). After washing four times, the membranes were incubated with Blocking One (Nacalai Tesque, Kyoto, Japan) for 1 hour at room temperature and overnight at 4°C with primary antibodies to β-actin (13E5), Met (25H2), phospho-Met (Y1234/Y1235;3D7), phospho-EGFR (Y1068), Akt, phospho-Akt (Ser473; 736E11), VEGFR-2 (55B11), phospho-VEGFR-2 (Tyr951;15D2), human EGFR (1 μg/ml), human/mouse/rat Erk1/Erk2 (0.2 μg/ml), and p-Erk1/Erk2 (T202/Y204; 0.1 μg/ml; R&D Systems). After three washes,

the membranes were incubated for 1 hour at room temperature with species-specific, horseradish peroxidase–conjugated secondary antibodies. Immunoreactive bands were visualized with Super Signal West Dura Extended Duration Substrate (Thermo Fisher Scientific, Waltham, MA) and an enhanced chemiluminescence substrate (Pierce Biotechnology, Rockford, IL). Each experiment was conducted at least three times independently.

Coculture of Lung Cancer Cells with Fibroblasts or Endothelial Cells

Cells were cocultured in Transwell collagen–coated chambers separated by an 8-mm (BD Biosciences, San Jose, CA) or 3-mm (Corning, Tewksbury, MA) pore size filter. Tumor cells (8×10^3 cells/800 ml) with or without TAS-115 (1.0 μmol/liter) or erlotinib (0.3 μmol/liter) in the lower chamber were cocultured with MRC-5 (1×10^4 cells/300 μl) cells in the upper chamber for 72 hours. The upper chamber was then removed, 200 μl of MTT solution was added to each well, and the cells were incubated for 2 hours at 37°C. The media was removed, and the dark blue crystals in each well were dissolved in 400 μl of dimethyl sulfoxide. Absorbance was measured with an MTP-120 Microplate reader (Corona Electric, Ibaraki, Japan) at test and reference wavelengths of 550 and 630 nm, respectively. The percentage of growth was measured relative to untreated controls. All samples were assayed at least in triplicate, with each experiment conducted three times independently.

Subcutaneous Xenograft Models

Nude mice (male, 5–6 weeks old) were obtained from Clea (Tokyo, Japan). Cultured tumor cells (PC-9/Vec or PC-9/HGF) were implanted subcutaneously into the flanks of each mouse at 3×10^6 cells/0.1 ml. When tumor volumes reached 100 to 200 mm^3, the mice (n = 5 per group) were randomized to the following groups: (1) no treatment (control group), (2) only 50 mg/kg of erlotinib orally, (3) only 25 mg/kg of crizotinib orally, (4) only 100 μg/mouse of bevacizumab intraperitoneally, (5) only 75 mg/kg of TAS-115 orally, (6) erlotinib and crizotinib, (7) crizotinib and bevacizumab, (8) erlotinib and bevacizumab, (9) erlotinib, crizotinib, and bevacizumab, and (10) erlotinib and TAS-115. Each tumor was measured in two dimensions three times a week, and the volume was calculated using the following formula: tumor volume (mm^3) = 1/2 (length (mm) × (width (mm))^2). All animal experiments complied with the Guidelines for the Institute for Experimental Animals, Kanazawa University Advanced Science Research Center (Approval No. AP-122505).

Histological Analyses

For detection of endothelial cells (CD31), 5-μm-thick frozen sections of xenograft tumors were fixed with cold acetone and washed with PBS. Then, endogenous peroxidase activity was blocked by incubation in 3% aqueous H_2O_2 for 10 minutes. After treatment with 5% normal horse serum, the sections were incubated with primary antibodies to mouse CD31 (MEC13.3; BD Biosciences). After probing with species-specific, biotinylated secondary antibodies, the sections were incubated for 30 minutes with avidin–biotinylated peroxidase complex by using a Vectastain ABC kit (Vector Laboratories, Burlingame, CA). The 3,3′-diaminobenzidine tetrahydrochloride Liquid System (DAKO, Glostrup, Denmark) was used to detect immunostaining. Omission of the primary antibody served as a negative control. Terminal deoxynucleotidyl transferase–mediated deoxyuridine triphosphate-biotin nick end-labeling staining was performed using the Apoptosis Detection System (Promega Corporation, Madison, WI). In brief, 5-μm-thick frozen sections of xenograft tumors were fixed with PBS containing 4% formalin. The slides were washed with PBS and permeabilized with 0.2% Triton X-100. The samples were then equilibrated, and DNA strand breaks were labeled with fluorescein-12-2-deoxy-uridine-5-triphosphate (fluorescein-12-dUTP) by adding the nucleotide mixture and the terminal deoxynucleotidyl transferase enzyme. The reaction was stopped with saline sodium citrate, and the localized green fluorescence of apoptotic cells was detected by fluorescence microscopy (×200). The five areas containing the highest numbers of stained cells within a section were selected for histologic quantitation by light or fluorescent microscopy at a ×400 magnification. All results were independently evaluated by three investigators (JN, TN, and ST).

Statistical Analysis

Differences were analyzed by one-way analysis of variance. All statistical analyses were carried out using GraphPad Prism Ver. 4.01 (GraphPad Software, Inc., La Jolla, CA). A p value of less than 0.01 was considered statistically significant.

RESULTS

Effect of Crizotinib and TAS-115 on Bypass Resistance Signals Triggered by Exogenous HGF In Vitro

In the first set of experiments, we examined the effect of crizotinib and TAS-115 on exogenously added HGF-triggered EGFR-TKI resistance in vitro. PC-9 and HCC827 cells are highly sensitive to erlotinib, whereas exogenously added HGF induces resistance to erlotinib in both cell lines. Crizotinib on its own discernibly inhibits the growth of PC-9 cell at high concentrations, consistent with its multikinase activities, and it remarkably sensitizes the cell to erlotinib even in the presence of HGF. TAS-115 does not affect the growth of PC-9 or HCC827 cells at concentrations less than 10 μmol/liter; however, the combined use of TAS-115 with erlotinib reverses HGF-induced resistance in the cell lines in a concentration-dependent manner (Figs. 1*A*, *B* and 2*A*, *B*, and Supplementary Figure 2, Supplementary Digital Content 2, http://links.lww.com/JTO/A571). We previously reported that stromal fibroblasts are a source of exogenous HGF for EGFR-TKI–naive NSCLC and that fibroblast-derived HGF induces resistance to gefitinib and erlotinib in PC-9 and HCC827 cells.[25] Crizotinib and TAS-115 reverse the erlotinib resistance of PC-9 cells induced by coculturing with MRC-5 cells (Supplementary Figure 3A, B, Supplementary Digital Content 3, http://links.lww.com/JTO/A572). These results indicate that both crizotinib and TAS-115 can reverse the EGFR-TKI resistance induced by exogenous HGF in vitro.

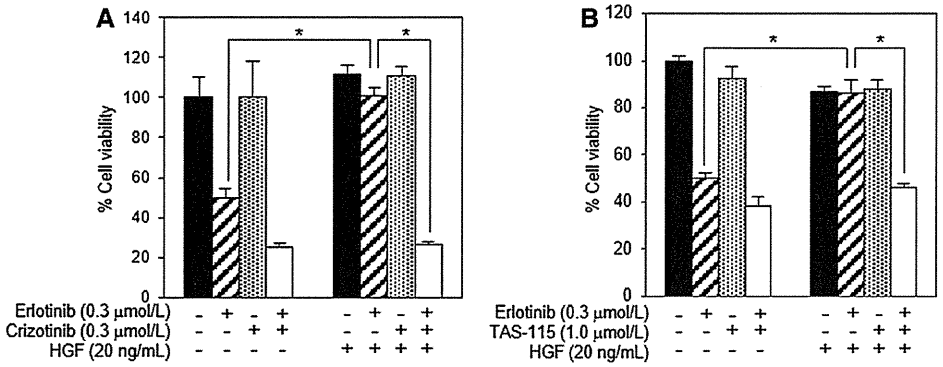

FIGURE 1. Combined use of crizotinib or TAS-115 with erlotinib reverses resistance to EGFR-TKI induced by exogenous HGF. *A* and *B*, PC-9 cells were incubated with or without erlotinib or crizotinib and TAS-115 in the presence or absence of HGF (20 ng/ml) for 72 hours. Cell viability was determined by MTT assay. Bars show SD. The data shown are representative of five independent experiments with similar results. EGFR, epidermal growth factor receptor; EGFR-TKI, EGFR-tyrosine kinase inhibitor; HGF, hepatocyte growth factor; MTT, Thiazolyl Blue Tetrazolium Bromide.

Effect of Crizotinib and TAS-115 on Bypass Resistance Signals Triggered by Endogenous HGF

Previously, we showed that HGF is predominantly present in tumor cells of patients with NSCLC with acquired resistance to EGFR-TKIs and that transient *HGF*-gene transfection into PC-9 cells results in resistance to EGFR-TKIs.[20] We, therefore, generated a stable *HGF*-gene transfectant in PC-9 cells (PC-9/HGF) and assessed the effects against continuously produced endogenous HGF. PC-9/HGF cells secrete high levels of HGF and become resistant to erlotinib, whereas PC-9 or the vector control PC-9/Vec cells do not. Although TAS-115 does not affect the growth of PC-9/HGF cells, crizotinib discernibly inhibits it at high concentrations. The combination of crizotinib or TAS-115 with erlotinib successfully reverses the resistance of PC-9/HGF cells (Fig. 2*A–G*). Using Western blotting, we examined the effects of crizotinib and TAS-115 on signal transduction in PC-9/Vec and PC-9/HGF cells (Fig. 2*H–I*). We found that erlotinib inhibits the phosphorylation of EGFR and ErbB3 in PC-9/Vec cells, thereby inhibiting the phosphorylation of Akt and extracellular signal-regulated kinase 1/2 (ERK1/2). Met phosphorylation is observed in PC-9/HGF cells but not in PC-9/Vec cells. However, erlotinib fails to inhibit phosphorylation of Akt or Erk1/2 in the presence of HGF. Both crizotinib and TAS-115 suppress the constitutive phosphorylation of Met but not EGFR, ErbB3, or downstream Akt and ERK1/2. HGF stimulates the phosphorylation of Met, but the combined use of crizotinib or TAS-115 with erlotinib inhibits the phosphorylation of Met, Akt, and Erk1/2. These results suggest that crizotinib and TAS-115, when combined with erlotinib, reverse HGF-triggered erlotinib resistance by inhibiting the Met/Gab1/PI3K/Akt pathway.

Effect of Crizotinib and TAS-115 on Angiogenesis In Vitro and In Vivo

As we reported previously,[21] exogenous and endogenous HGF stimulated VEGF production in the PC-9 cancer cell line. Both crizotinib and TAS-115 inhibit VEGF production, presumably because of inhibiting Met activation by HGF (Fig. 3*A, B*). We also assessed the effect of crizotinib, TAS-115, and bevacizumab on the growth of HMVECs. VEGF promoted HMVEC viability, whereas TAS-115 and bevacizumab, but not crizotinib, inhibit VEGF-stimulated viability of HMVECs in a dose-dependent manner (Fig. 3*C, D*). We also explored the potential of TAS-115 against VEGFR-2. Western blot analysis indicated that VEGFR-2 is phosphorylated by VEGF stimulation in HMVECs, and TAS-115 and bevacizumab show an inhibitory effect (Supplementary Figure 4, Supplementary Digital Content 4, http://links.lww.com/JTO/A573). We next examined the effect on in vivo angiogenesis by using short-term treatment models. Nude mice with established subcutaneous tumors (tumor volume approximately 100 mm^3) were treated with erlotinib with or without crizotinib, bevacizumab, and/or TAS-115, and tumor vascularization was determined on day 4 (Fig. 4*A, B*). In PC-9/Vec tumors, treatment with erlotinib alone, TAS-115 alone, or erlotinib with TAS-115 inhibited vascularization. PC-9/HGF tumors have more vascularization than PC-9/Vec tumors. In PC-9/HGF tumors, treatment with bevacizumab, but not erlotinib or crizotinib, inhibited vascularization. We found that TAS-115 inhibited vascularization more potently than bevacizumab. Under these experimental conditions, treatment with erlotinib plus crizotinib inhibited vascularization. Importantly, erlotinib plus TAS-115 more potently inhibited vascularization, compared with erlotinib plus crizotinib, with or without bevacizumab. These results indicate that TAS-115 has a high potential to inhibit angiogenesis in vivo in *EGFR*-mutant tumors that produce high levels of HGF. We also confirmed that treatment with crizotinib or TAS-115 inhibits the phosphorylation of EGFR and Met in vivo (Supplementary Figure 5, Supplementary Digital Content 5, http://links.lww.com/JTO/A574).

Effect of Combined Treatment on Growth of HGF-Overexpressing Tumors In Vivo

Nude mice bearing established subcutaneous tumors (tumor volume approximately 100 mm^3) were treated with erlotinib with or without crizotinib, bevacizumab, and/or TAS-115 for 39 days. The treatment was feasible, and no

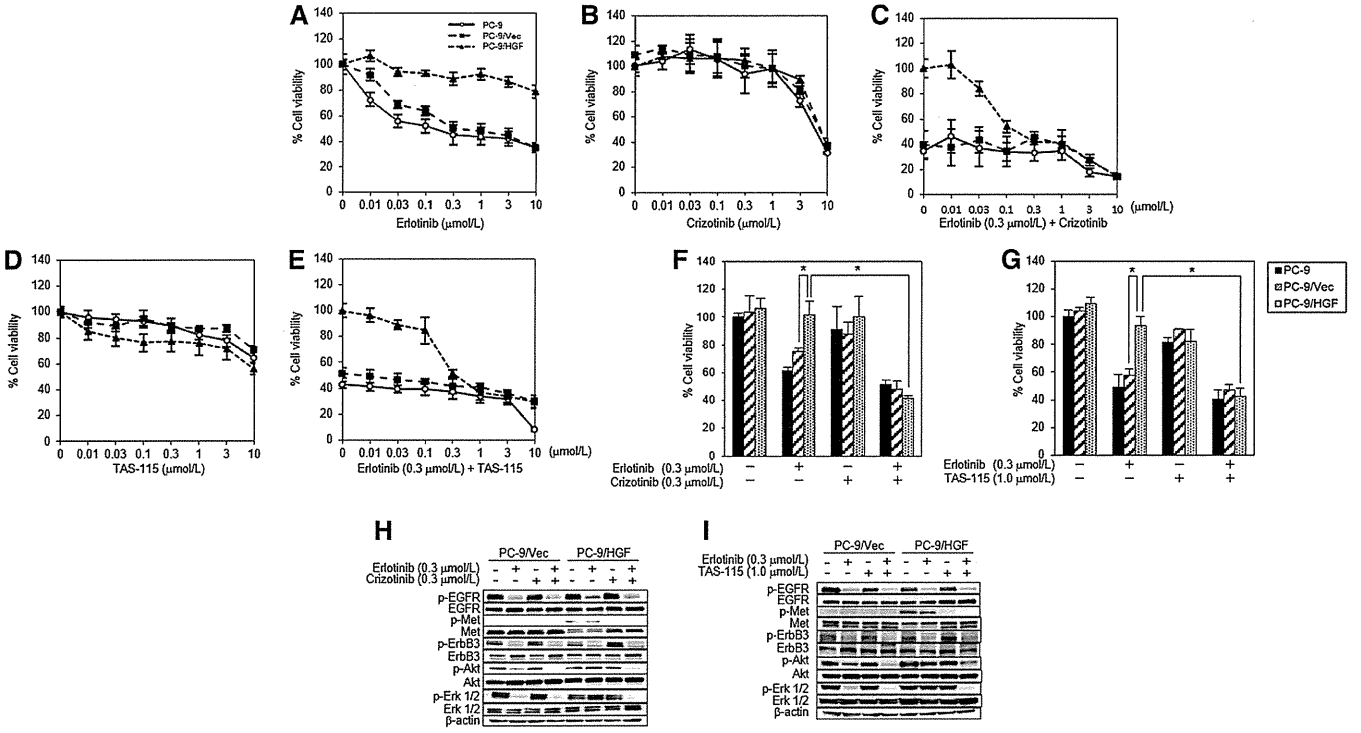

FIGURE 2. Combined use of crizotinib or TAS-115 with erlotinib reverses resistance to EGFR-TKI induced by endogenous HGF. *A*, PC-9/Vec and PC-9/HGF cells were incubated with or without erlotinib for 72 hours. Cell viability was determined by MTT assay. Bars show SD. *B* and *D*, PC-9/Vec and PC-9/HGF cells were treated with crizotinib or TAS-115 for 72 hours. *C–G*, PC-9/Vec and PC-9/HGF cells were incubated with or without erlotinib (0.3 μmol/liter) with or without crizotinib (0.3 μmol/liter) and TAS-115 (1.0 μmol/liter) for 72 hours. The data shown are from three independent experiments with similar results. *H* and *I*, PC-9/HGF cells were incubated with TAS-115 (1.0 μmol/liter) or crizotinib (0.3 μmol/liter) and/or erlotinib (0.3 μmol/liter) for 1 hour. Thereafter, cell lysates were harvested, and phosphorylation of the indicated proteins was determined by Western blot analysis. EGFR, epidermal growth factor receptor; EGFR-TKI, EGFR-tyrosine kinase inhibitor; HGF, hepatocyte growth factor; MTT, thiazolyl blue tetrazolium bromide.

adverse events, including loss of weight, were observed. Tumor volumes on day 39 are shown in Figure 5*A* and *B* (tumor growth curves over time are shown in Supplementary Figure 6, Supplementary Digital Content 6, http://links.lww.com/JTO/A575). Erlotinib markedly inhibited the growth of PC-9/Vec tumors, but TAS-115 inhibited it only modestly (81.7% and 40%, respectively). In PC-9/HGF tumors, erlotinib alone and crizotinib alone inhibited tumor growth only slightly (30% and 31.9%, respectively). Moreover, bevacizumab alone and TAS-115 alone inhibited tumor growth modestly (67% and 76.6%, respectively). Erlotinib plus crizotinib, with or without bevacizumab, inhibited tumor growth markedly (87.1% and 88.3%, respectively). Importantly, erlotinib plus TAS-115 further inhibited tumor growth significantly (93.7%).

Effect of Combined Treatment on Regrowth of HGF-Overexpressing Tumors after Cessation of the Treatment

We further evaluated the effect on regrowth of PC-9/HGF tumors after cessation of drug treatment. After 10 days of cessation, tumors treated with erlotinib plus crizotinib with or without bevacizumab regrew to 4.5 and 3.3 times their initial size at the start of cessation, respectively. Tumors treated with erlotinib plus TAS-115 regrew to only 1.7 times their initial size (Fig. 6*A*). To explore the mechanism of this phenomenon, we again evaluated tumor vascularization on day 49 (10 days after the start of cessation). Consistent with an inhibitory effect against tumor regrowth, vessel density was high (104.6±7.3) and modest (68.6±8.0) in tumors treated with erlotinib plus crizotinib without and with bevacizumab, respectively, whereas vessel density in the tumors treated with erlotinib plus TAS-115 was very low (37.8±3.5; Fig. 6*B*). However, the number of apoptotic cells was low (1.5±0.6), modest (7.3±5.7), and high (22.7±6.4) in the tumors treated with erlotinib plus crizotinib, crizotinib and bevacizumab, and TAS-115, respectively. These results suggest that erlotinib plus TAS-115 prevents tumor regrowth, even after cessation, by means of sustained inhibition of angiogenesis.

DISCUSSION

In the present study, we demonstrated that combined use of erlotinib and TAS-115, a novel angiogenesis inhibitor with Met inhibitory activity, and the use of a triplet of clinically available drugs (such as erlotinib, crizotinib, and bevacizumab) could inhibit the growth of HGF-triggered EGFR-TKI–resistant tumors containing *EGFR* mutations.

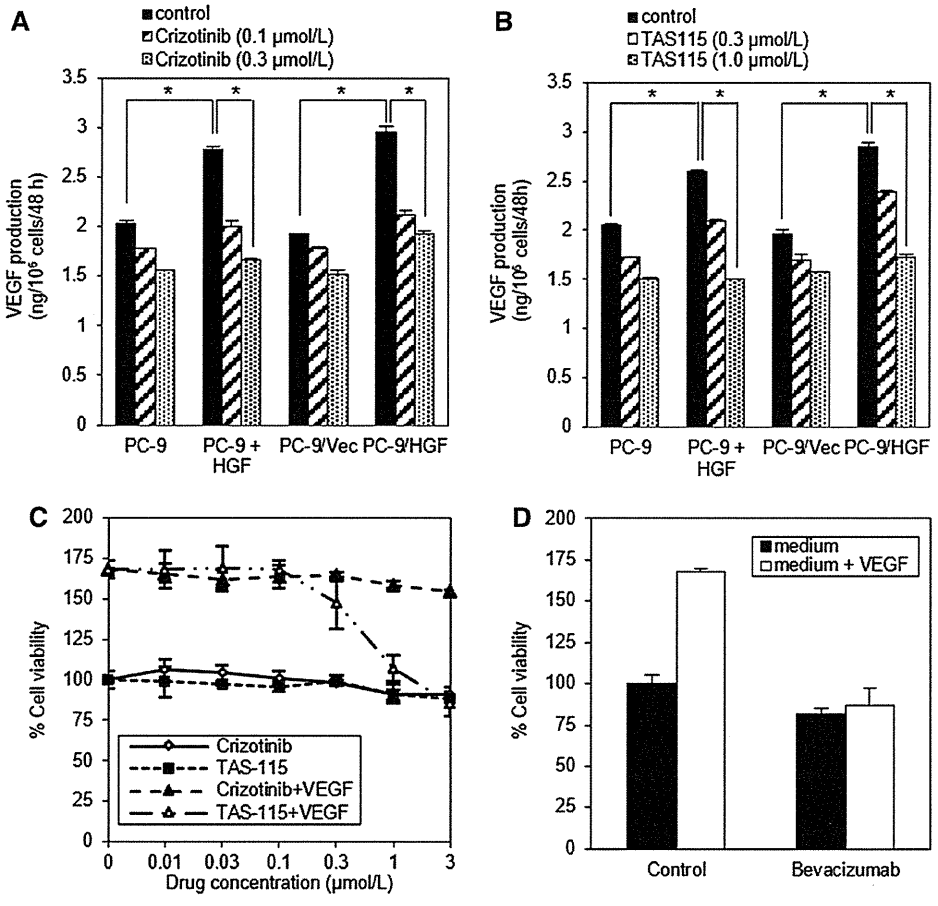

FIGURE 3. Crizotinib and TAS-115 inhibits VEGF production by cancer cells and endothelial proliferation. *A* and *B*, Tumor cells were incubated with or without HGF (50 ng/ml) in the presence of different concentrations of crizotinib or TAS-115 for 48 hours. Thereafter, supernatants were harvested, and the number of tumor cells was counted. VEGF concentration in the supernatants was determined by ELISA. VEGF levels corrected by the tumor cell number are shown. C and D, HMVECs were incubated in RPMI-1640 medium with 10% FBS (control) or RPMI-1640 medium with 10% FBS in the presence or absence of VEGF (50 ng/ml) with different concentrations of TAS-115, crizotinib, or bevacizumab for 72 hours. Thereafter, cell viability was determined by MTT assay. Bars show SD. The data shown are from three independent experiments with similar results. VEGF, vascular endothelial growth factor; HGF, hepatocyte growth factor; ELISA, enzyme-linked immunosorbent assay; HMVECs, human dermal microvascular endothelial cells; FBS, fetal bovine serum; MTT, thiazolyl blue tetrazolium bromide.

Moreover, TAS-115 combined with erlotinib remarkably delayed the regrowth of the HGF-triggered EGFR-TKI–resistant tumors.

Because we reported that HGF is a resistance factor to EGFR-TKI in *EGFR*-mutant lung cancer,[9] HGF has been shown to induce resistance to various molecularly targeted drugs in different types of cancers with driver oncogenes. HGF causes resistance to a selective ALK inhibitor[26] and a BRAF inhibitor[27] in lung cancer with *ALK* rearrangement and melanoma with *BRAF* mutation, respectively, by inducing bypass signals that trigger resistance. Moreover, HGF restores angiogenesis associated with Met expression in tumor vascular endothelial cells and thus induces resistance to sunitinib in various types of cancer.[28] These observations indicate that HGF induces resistance to molecularly targeted drugs by multiple mechanisms; therefore, it is an important therapeutic target for circumventing resistance to various molecularly targeted drugs.

HGF and its receptor Met have a close relation with VEGF. Anti-VEGF treatment resulted in a remarkable up-regulation of Met expression in tumors.[29] Hypoxia-stimulated expression of VEGF,[30] Met,[29] and Neuropilin1 (NRP1), a receptor of VEGF, promotes tumor progression.[29,31] Furthermore, it was reported that serum levels of HGF and VEGF were inversely correlated with the clinical response to EGFR-TKIs in lung cancer.[32–34] In addition, a dual inhibitor of VEGFR-2 and Met (XL-184) was shown to have completely suppressed the invasion and metastasis in a pancreatic cancer model in vivo.[29] These studies indicate the rationale for simultaneous inhibition of the HGF-Met and VEGF/VEGFR-2 axes for cancer therapy.

In line with our previous results, we observed that inhibition of both the driver signal (EGFR) and the resistance signal (Met) remarkably suppressed the growth of HGF-triggered EGFR-TKI–resistant tumors in vivo. However, the tumors regrew immediately after the cessation of the dual inhibition, which indicated the presence of cancer cells with proliferating potential that persisted continuously throughout the dual inhibition. Mechanisms of the resistance to dual inhibition should be clarified in the near future.

Additional inhibition of angiogenesis by VEGF neutralization or VEGFR inhibition in addition to dual inhibition (EGFR and Met) could further inhibit growth of HGF-triggered EGFR-TKI–resistant tumor and delay regrowth of the tumors after cessation of the treatment. Bevacizumab in combination with cytotoxic chemotherapy has been shown to prolong progression-free survival in various solid tumors. Our results suggest that the angiogenesis inhibitor in combination with molecularly targeted drugs such as EGFR-TKI and Met-TKI, which directly act on cancer cells, may also delay tumor progression.

It is still controversial whether tumor blood vessels rapidly regrow after cessation of VEGF inhibition. Mancuso et al.[35] reported that tumor vasculature regrew within 7 days of

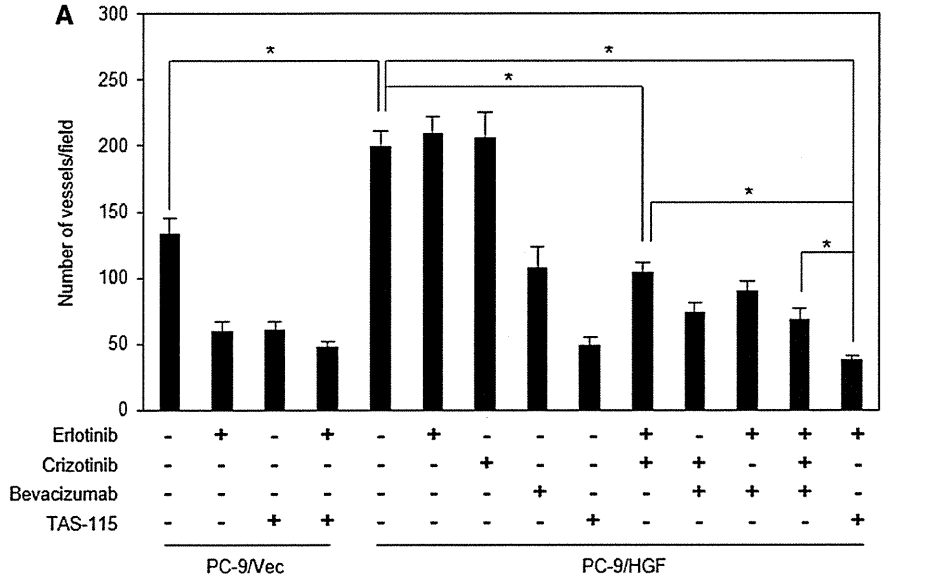

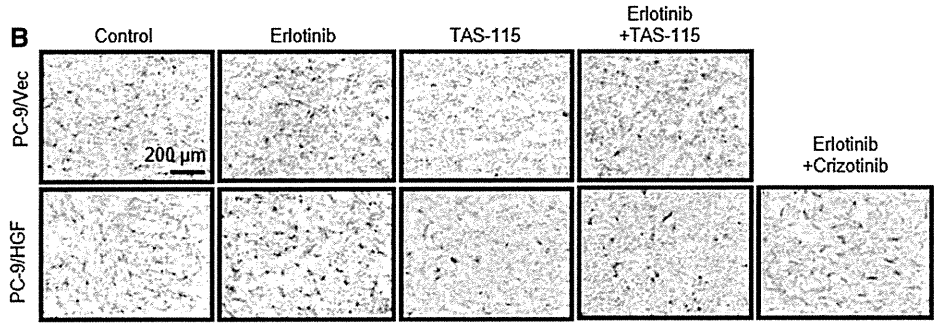

FIGURE 4. Treatment with erlotinib plus TAS-115 inhibits angiogenesis in PC-9/HGF tumors in vivo. Nude mice bearing PC-9/Vec or PC-9/HGF tumors (approximately 100 mm^3 in size) were administered erlotinib and/or crizotinib and/or TAS-115 orally, once daily for 4 days, and/or bevacizumab intraperitoneally only once. *A*, The mice were killed on day 4, and the tumors were harvested. *B*, Numbers of tumor vessels (mean ± SE) determined by CD31 immunohistochemical staining are shown for groups containing five mice each. Representative graphs are shown. The data shown are representative of two independent experiments with similar results. HGF, hepatocyte growth factor.

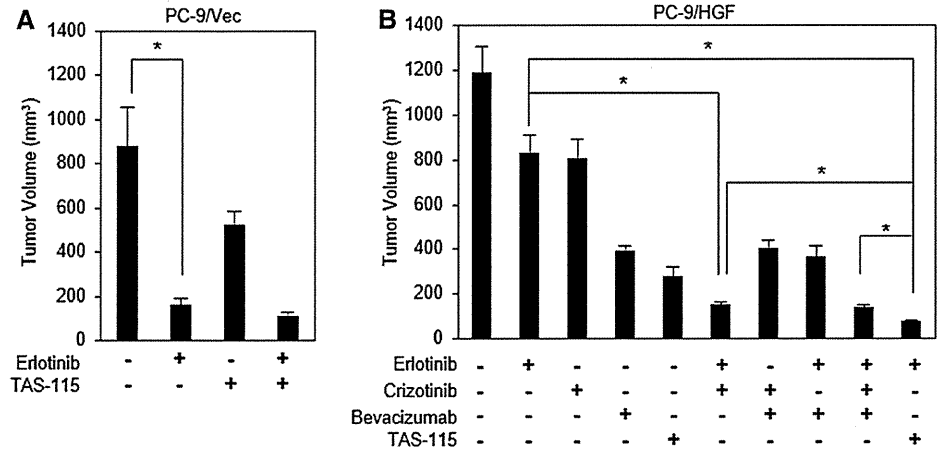

FIGURE 5. Treatment with erlotinib plus TAS-115 inhibits the growth of PC-9/HGF tumors in vivo. *A* and *B*, Nude mice bearing PC-9/Vec or PC-9/HGF tumors (approximately 100 mm^3 in size) were administered erlotinib and/or crizotinib and/or TAS-115 orally once daily and/or bevacizumab intraperitoneally once a week. Tumor volume was measured using calipers. Mean ± SE tumor volumes on day 39 are shown for groups containing five mice each. The data shown are representative of two independent experiments with similar results. HGF, hepatocyte growth factor.

cessation of VEGFR inhibitors (given for 7 days) in the RIP-Tag2 pancreatic cancer model and the Lewis lung carcinoma-xenograft model. Bagri et al.[36] showed that long-term (7 weeks) treatment with an anti-VEGF antibody prevented the regrowth of tumors compared with control or short-term (2 weeks) treatment, but the effect of the long-term treatment on vasculature regrowth after cessation was not well elucidated. In the present study, we demonstrated that regrowth of tumor vasculature was inhibited even after cessation for 10 days of treatment when, before that, continuous treatment (for 39 days) consisted of bevacizumab plus erlotinib and crizotinib or TAS-115 plus erlotinib; and this inhibition was associated with a high number of apoptotic cells in the tumors and delayed tumor regrowth. These effects were more remarkable with TAS-115 plus erlotinib than with the triplet treatment in our experimental conditions. It is unclear why continuous triple inhibition, especially by TAS-115 plus erlotinib, delayed the recovery of tumor angiogenesis. One possible explanation is that continuous treatment with

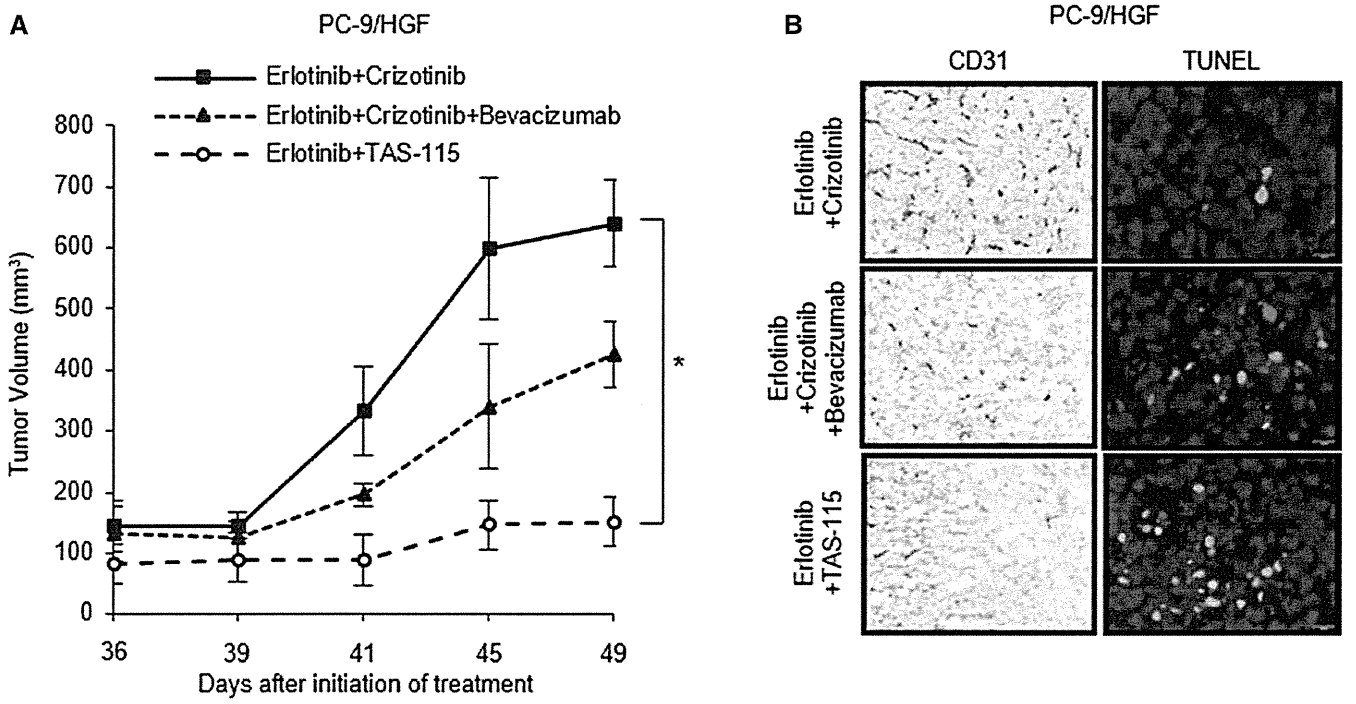

FIGURE 6. Treatment with erlotinib plus TAS-115 most strongly prevented the regrowth of PC-9/HGF tumors even after cessation of treatment. *A*, Nude mice bearing PC-9/HGF tumors were treated as described in Figure 5 until day 39. Thereafter, treatment was terminated, and tumor volume was measured until day 49. *B*, The mice were killed on day 49, and tumors were harvested. Tumor vessels and apoptotic cells were determined by CD31 immunohistochemical and TUNEL staining, respectively. Asterisk indicates $P < 0.01$. HGF, hepatocyte growth factor; TUNEL, terminal deoxynucleotidyl transferase–mediated deoxyuridine triphosphate-biotin nick end-labeling.

TAS-115 may impair the function of endothelial progenitor cells expressing VEGFR-2. Further studies with longer follow-up and histochemical analysis will be required to determine the exact mechanisms. On the other hand, VEGFR inhibitory activity may be the disadvantage of TAS-115 for specific cases in which EGFR-TKI resistance caused by only MET amplification. Previous study reported that anti-VEGF therapy elicits malignant progression of tumors to increased local invasion and distant metastasis.[37] Therefore, biomarkers for detecting the activities of MET and VEGFRs may be necessary for the optimal use of dual inhibitors for MET and VEGFR.

Inhibition of multiple signaling pathways may cause severe adverse events, especially with continuous admiration of the inhibitors. In our study, 50 mg/kg erlotinib administered daily plus 100 μg/body bevacizumab administered weekly did not show obvious adverse events in nude mice. However, some nude mice treated with daily 50 mg/kg crizotinib plus daily 50 mg/kg erlotinib exhibited severe weight loss and died. Thus, we had to reduce the dose of crizotinib to 25 mg/kg daily when administered along with 50 mg/kg erlotinib. On the other hand, daily administration of 75 mg/kg TAS-115, as expected, inhibited its two targets, Met phosphorylation and angiogenesis, in vivo, and did not show obvious adverse events, including weight loss, even in combination with daily administration of 50 mg/kg erlotinib, suggesting the feasibility of this combined treatment. However, the safety and efficacy of triple inhibition with the triplet of clinically available drugs or with erlotinib plus TAS-115 need to be carefully evaluated in clinical trials.

In conclusion, we demonstrated that triple inhibition of EGFR, Met, and angiogenesis could be achieved by a combination of clinically available drugs (erlotinib, crizotinib, and bevacizumab) or erlotinib and TAS-115 and that the triple inhibition efficiently controlled growth of HGF-triggered, EGFR-TKI–resistant tumors containing *EGFR* mutations. Clinical trials are warranted to evaluate the efficacy and safety of the triple inhibition in *EGFR*-mutant lung cancer patients who acquired EGFR-TKI resistance due to HGF.

ACKNOWLEDGMENTS

This study was supported by Grants-in-Aid for Cancer Research (21390256 to Dr. Yano); Scientific Research on Innovative Areas "Integrative Research on Cancer Microenvironment Network" from the Ministry of Education, Culture, Sports, Science, and Technology of Japan (22112010A01 to Dr. Yano); and Taiho Pharmaceutical, Co. Ltd.

REFERENCES

1. Lynch TJ, Bell DW, Sordella R, et al. Activating mutations in the epidermal growth factor receptor underlying responsiveness of non-small-cell lung cancer to gefitinib. *N Engl J Med* 2004;350:2129–2139.
2. Paez JG, Jänne PA, Lee JC, et al. EGFR mutations in lung cancer: correlation with clinical response to gefitinib therapy. *Science* 2004;304:1497–1500.
3. Pao W, Miller V, Zakowski M, et al. EGF receptor gene mutations are common in lung cancers from "never smokers" and are associated with

sensitivity of tumors to gefitinib and erlotinib. *Proc Natl Acad Sci U S A* 2004;101:13306–13311.
4. Jackman D, Pao W, Riely GJ, et al. Clinical definition of acquired resistance to epidermal growth factor receptor tyrosine kinase inhibitors in non-small-cell lung cancer. *J Clin Oncol* 2010;28:357–360.
5. Pao W, Chmielecki J. Rational, biologically based treatment of EGFR-mutant non-small-cell lung cancer. *Nat Rev Cancer* 2010;10:760–774.
6. Kobayashi S, Boggon TJ, Dayaram T, et al. EGFR mutation and resistance of non-small-cell lung cancer to gefitinib. *N Engl J Med* 2005;352:786–792.
7. Pao W, Miller VA, Politi KA, et al. Acquired resistance of lung adenocarcinomas to gefitinib or erlotinib is associated with a second mutation in the EGFR kinase domain. *PLoS Med* 2005;2:e73.
8. Engelman JA, Zejnullahu K, Mitsudomi T, et al. MET amplification leads to gefitinib resistance in lung cancer by activating ERBB3 signaling. *Science* 2007;316:1039–1043.
9. Yano S, Wang W, Li Q, et al. Hepatocyte growth factor induces gefitinib resistance of lung adenocarcinoma with epidermal growth factor receptor-activating mutations. *Cancer Res* 2008;68:9479–9487.
10. Bivona TG, Hieronymus H, Parker J, et al. FAS and NF-κB signalling modulate dependence of lung cancers on mutant EGFR. *Nature* 2011;471:523–526.
11. Zhang Z, Lee JC, Lin L, et al. Activation of the AXL kinase causes resistance to EGFR-targeted therapy in lung cancer. *Nat Genet* 2012;44:852–860.
12. Zakowski MF, Ladanyi M, Kris MG; Memorial Sloan-Kettering Cancer Center Lung Cancer OncoGenome Group. EGFR mutations in small-cell lung cancers in patients who have never smoked. *N Engl J Med* 2006;355:213–215.
13. Morinaga R, Okamoto I, Furuta K, et al. Sequential occurrence of non-small cell and small cell lung cancer with the same EGFR mutation. *Lung Cancer* 2007;58:411–413.
14. Shiao TH, Chang YL, Yu CJ, et al. Epidermal growth factor receptor mutations in small cell lung cancer: a brief report. *J Thorac Oncol* 2011;6:195–198.
15. Frederick BA, Helfrich BA, Coldren CD, et al. Epithelial to mesenchymal transition predicts gefitinib resistance in cell lines of head and neck squamous cell carcinoma and non-small cell lung carcinoma. *Mol Cancer Ther* 2007;6:1683–1691.
16. Uramoto H, Iwata T, Onitsuka T, Shimokawa H, Hanagiri T, Oyama T. Epithelial-mesenchymal transition in EGFR-TKI acquired resistant lung adenocarcinoma. *Anticancer Res* 2010;30:2513–2517.
17. Suda K, Tomizawa K, Fujii M, et al. Epithelial to mesenchymal transition in an epidermal growth factor receptor-mutant lung cancer cell line with acquired resistance to erlotinib. *J Thorac Oncol* 2011;6:1152–1161.
18. Garofalo M, Romano G, Di Leva G, et al. EGFR and MET receptor tyrosine kinase-altered microRNA expression induces tumorigenesis and gefitinib resistance in lung cancers. *Nat Med* 2012;18:74–82.
19. Huang S, Hölzel M, Knijnenburg T, et al. MED12 controls the response to multiple cancer drugs through regulation of TGF-β receptor signaling. *Cell* 2012;151:937–950.
20. Yano S, Takeuchi S, Nakagawa T, Yamada T. Ligand-triggered resistance to molecular targeted drugs in lung cancer: roles of hepatocyte growth factor and epidermal growth factor receptor ligands. *Cancer Sci* 2012;103:1189–1194.
21. Takeuchi S, Wang W, Li Q, et al. Dual inhibition of Met kinase and angiogenesis to overcome HGF-induced EGFR-TKI resistance in EGFR mutant lung cancer. *Am J Pathol* 2012;181:1034–1043.
22. Kwak EL, Bang YJ, Camidge DR, et al. Anaplastic lymphoma kinase inhibition in non-small-cell lung cancer. *N Engl J Med* 2010;363:1693–1703.
23. Bergethon K, Shaw AT, Ou SH, et al. ROS1 rearrangements define a unique molecular class of lung cancers. *J Clin Oncol* 2012;30:863–870.
24. Nakagawa T, Takeuchi S, Yamada T, et al. Combined therapy with mutant-selective EGFR inhibitor and Met kinase inhibitor for overcoming erlotinib resistance in EGFR-mutant lung cancer. *Mol Cancer Ther* 2012;11:2149–2157.
25. Yamada T, Matsumoto K, Wang W, et al. Hepatocyte growth factor reduces susceptibility to an irreversible epidermal growth factor receptor inhibitor in EGFR-T790M mutant lung cancer. *Clin Cancer Res* 2010;16:174–183.
26. Yamada T, Takeuchi S, Nakade J, et al. Paracrine receptor activation by microenvironment triggers bypass survival signals and ALK inhibitor resistance in EML4-ALK lung cancer cells. *Clin Cancer Res* 2012;18:3592–3602.
27. Wilson TR, Fridlyand J, Yan Y, et al. Widespread potential for growth-factor-driven resistance to anticancer kinase inhibitors. *Nature* 2012;487:505–509.
28. Shojaei F, Lee JH, Simmons BH, et al. HGF/c-Met acts as an alternative angiogenic pathway in sunitinib-resistant tumors. *Cancer Res* 2010;70:10090–10100.
29. Sennino B, Ishiguro-Oonuma T, Wei Y, et al. Suppression of tumor invasion and metastasis by concurrent inhibition of c-Met and VEGF signaling in pancreatic neuroendocrine tumors. *Cancer Discov* 2012;2:270–287.
30. Endoh H, Yatabe Y, Kosaka T, Kuwano H, Mitsudomi T. PTEN and PIK3CA expression is associated with prolonged survival after gefitinib treatment in EGFR-mutated lung cancer patients. *J Thorac Oncol* 2006;1:629–634.
31. Zhang S, Zhau HE, Osunkoya AO, et al. Vascular endothelial growth factor regulates myeloid cell leukemia-1 expression through neuropilin-1-dependent activation of c-MET signaling in human prostate cancer cells. *Mol Cancer* 2010;9:9.
32. Kasahara K, Arao T, Sakai K, et al. Impact of serum hepatocyte growth factor on treatment response to epidermal growth factor receptor tyrosine kinase inhibitors in patients with non-small cell lung adenocarcinoma. *Clin Cancer Res* 2010;16:4616–4624.
33. Tanaka H, Kimura T, Kudoh S, et al. Reaction of plasma hepatocyte growth factor levels in non-small cell lung cancer patients treated with EGFR-TKIs. *Int J Cancer* 2011;129:1410–1416.
34. Han JY, Kim JY, Lee SH, Yoo NJ, Choi BG. Association between plasma hepatocyte growth factor and gefitinib resistance in patients with advanced non-small cell lung cancer. *Lung Cancer* 2011;74:293–299.
35. Mancuso MR, Davis R, Norberg SM, et al. Rapid vascular regrowth in tumors after reversal of VEGF inhibition. *J Clin Invest* 2006;116:2610–2621.
36. Bagri A, Berry L, Gunter B, et al. Effects of anti-VEGF treatment duration on tumor growth, tumor regrowth, and treatment efficacy. *Clin Cancer Res* 2010;16:3887–3900.
37. Pàez-Ribes M, Allen E, Hudock J, et al. Antiangiogenic therapy elicits malignant progression of tumors to increased local invasion and distant metastasis. *Cancer Cell* 2009;15:220–231.

Published OnlineFirst October 28, 2014; DOI: 10.1158/1078-0432.CCR-14-1385

Cancer Therapy: Preclinical

Clinical Cancer Research

Cabozantinib Overcomes Crizotinib Resistance in ROS1 Fusion–Positive Cancer

Ryohei Katayama[1], Yuka Kobayashi[1,2], Luc Friboulet[3,4], Elizabeth L. Lockerman[3,4], Sumie Koike[1], Alice T. Shaw[3,4], Jeffrey A. Engelman[3,4], and Naoya Fujita[1,2]

Abstract

Purpose: *ROS1* rearrangement leads to constitutive ROS1 activation with potent transforming activity. In an ongoing phase I trial, the ALK tyrosine kinase inhibitor (TKI) crizotinib shows remarkable initial responses in patients with non–small cell lung cancer (NSCLC) harboring *ROS1* fusions; however, cancers eventually develop crizotinib resistance due to acquired mutations such as G2032R in ROS1. Thus, understanding the crizotinib-resistance mechanisms in *ROS1*-rearranged NSCLC and identification of therapeutic strategies to overcome the resistance are required.

Experimental Design: The sensitivity of CD74–ROS1–transformed Ba/F3 cells to multiple ALK inhibitors was examined. Acquired ROS1 inhibitor–resistant mutations in CD74–ROS1 fusion were screened by *N*-ethyl-*N*-nitrosourea mutagenesis with Ba/F3 cells. To overcome the resistance mutation, we performed high-throughput drug screening with small-molecular inhibitors and anticancer drugs used in clinical practice or being currently tested in clinical trials. The effect of the identified drug was assessed in the CD74–ROS1–mutant Ba/F3 cells and crizotinib-resistant patient-derived cancer cells (MGH047) harboring G2032R-mutated CD74–ROS1.

Results: We identified multiple novel crizotinib-resistance mutations in the ROS1 kinase domain, including the G2032R mutation. As the result of high-throughput drug screening, we found that the cMET/RET/VEGFR inhibitor cabozantinib (XL184) effectively inhibited the survival of CD74–ROS1 wild-type (WT) and resistant mutants harboring Ba/F3 and MGH047 cells. Furthermore, cabozantinib could overcome all the resistance by all newly identified secondary mutations.

Conclusions: We developed a comprehensive model of acquired resistance to ROS1 inhibitors in NSCLC with *ROS1* rearrangement and identified cabozantinib as a therapeutic strategy to overcome the resistance. *Clin Cancer Res; 21(1); 166–74. ©2014 AACR.*

Introduction

An increasing number of genetic alterations that aberrantly activate tyrosine kinases have been identified as oncogenic drivers of non–small cell lung cancer (NSCLC). Active mutations of epidermal growth factor receptor (EGFR), such as the L858R point mutation or deletion/insertion of several amino acids between exons 19 and 20, are more commonly observed in patients with NSCLC. The active mutation of KRAS is also predominantly found in patients with NSCLC. In addition to these active oncogene mutations, chromosomal rearrangements involving the tyrosine kinase domains of *ALK*, *ROS1*, and *RET* are observed in 1% to 5% of patients with NSCLC (1). The oncogenic fusion protein in NSCLC can be targeted by tyrosine kinase inhibitors (TKI), such as crizotinib; therefore, a number of specific TKIs targeting the fusion tyrosine kinase are currently under development. Although EGFR inhibitors (e.g., gefitinib or erlotinib) or the ALK inhibitor crizotinib show remarkable efficacy in most cases, the majority of patients will develop tumors resistant to targeted therapies in less than 1 year of treatment (2, 3). In cancers harboring the ALK fusion protein, several mechanisms of crizotinib resistance have been reported, including acquired secondary mutations in the kinase domain of ALK, genomic amplification of the *ALK* fusion gene, and amplification or activation of other kinases (3–7).

Recently, crizotinib was shown to be an effective inhibitor of ROS1 tyrosine kinase, and two case reports have described the activity of crizotinib in patients with *ROS1*-rearranged lung cancers (8, 9). Although crizotinib exhibited activity in a patient with NSCLC harboring the *ROS1* fusion, a resistant tumor eventually emerged. Recently, the G2032R mutation in the ROS1 kinase domain was identified in a crizotinib-treated resistant tumor, which was not observed before treatment (10). The mutation was located in the solvent-front region of the ROS1 kinase domain and was analogous to the G1202R ALK mutation identified in crizotinib-resistant ALK-rearranged lung cancers. We previously reported that the ALK G1202R mutation confers high-level resistance to crizotinib compared with all next-generation ALK inhibitors that were examined (3). Therefore, it is important to identify novel compounds that can overcome the G2032R ROS1 mutation, which confers crizotinib resistance in these cancers.

[1]Division of Experimental Chemotherapy, Cancer Chemotherapy Center, Japanese Foundation for Cancer Research, Tokyo, Japan. [2]Department of Medical Genome Science, Graduate School of Frontier Science, The University of Tokyo, Tokyo, Japan. [3]Massachusetts General Hospital Cancer Center, Boston, Massachusetts. [4]Department of Medicine, Harvard Medical School, Boston, Massachusetts.

Note: Supplementary data for this article are available at Clinical Cancer Research Online (http://clincancerres.aacrjournals.org/).

Corresponding Author: Naoya Fujita, Cancer Chemotherapy Center, Japanese Foundation for Cancer Research, 3-8-31, Ariake, Koto-ku, Tokyo 135-8550, Japan. Phone: 81-3-3520-0111; Fax: 81-3-3570-0484; E-mail: naoya.fujita@jfcr.or.jp

doi: 10.1158/1078-0432.CCR-14-1385

Published OnlineFirst October 28, 2014; DOI: 10.1158/1078-0432.CCR-14-1385

Translational Relevance

ROS1 gene rearrangement leads to constitutive ROS1 activation with potent transforming activity. Although crizotinib shows remarkable initial responses, cancers eventually develop resistance to crizotinib. To identify further mechanisms of resistance to crizotinib, we performed *N*-ethyl-*N*-nitrosourea (ENU) mutagenesis screening using CD74–ROS1–expressing Ba/F3 cells, and identified several novel crizotinib-resistance mutations in the ROS1 kinase domain, including the G2032R mutation, which is observed in the crizotinib-resistant patient. To overcome the identified crizotinib resistance, we performed high-throughput drug screening, and found that the cMET/RET/VEGFR inhibitor cabozantinib (XL184) effectively inhibited the survival of both wild-type (WT) and crizotinib-resistant mutated CD74–ROS1–expressing Ba/F3 cells. Because cabozantinib (XL184) is clinically available for the treatment of patients with thyroid cancer, the finding that cabozantinib can overcome the crizotinib resistances caused by secondary mutations in ROS1 potentially could change the therapeutic strategies for *ROS1*-rearranged non–small cell lung cancer (NSCLC).

In this study, we tested several ALK inhibitors to examine the potency of the sterically distinct ALK inhibitors, because the kinase domains of ALK and ROS1 are highly similar and grouped in the same kinase family (11). Subsequently, we identified a number of different crizotinib and/or ceritinib resistant mutations including G2032R mutation in the ROS1 kinase domain by *N*-ethyl-*N*-nitrosourea (ENU)–driven accelerated mutagenesis screening. High-throughput drug screening identified several kinase inhibitors as a potent ROS1 inhibitor, and identified that the cMET/RET/vascular endothelial growth factor (VEGFR) inhibitor cabozantinib can potently inhibit both wild-type (WT) and the resistant mutant CD74–ROS1. On the basis of these results, we propose the use of several inhibitors as alternative therapeutic strategies for ROS1-rearranged cancers and cabozantinib as a key drug for overcoming crizotinib resistance in ROS1 fusion–positive cancer cells lines, particularly those mediated by secondary mutations.

Materials and Methods

Reagents

Crizotinib was obtained from ShangHai Biochempartner; alectinib, cabozantinib, and ceritinib (LDK378) were purchased from ActiveBiochem; NVP-TAE-684 and ASP3026 were purchased from ChemieTek; AP26113 was purchased from Selleck; and foretinib was purchased from AdooQ BioScience. Each compound was dissolved in dimethyl sulfoxide (DMSO) for cell culture experiments. For inhibitor screening, the SCADS Inhibitor Kit was provided by the Screening Committee of Anticancer Drugs supported by a Grant-in-Aid for Scientific Research on Innovative Areas, Scientific Support Programs for Cancer Research, from the Ministry of Education, Culture, Sports, Science, and Technology of Japan.

Isolation of genomic DNA, preparation of total RNA, and sequencing of the *ROS1* fusion gene

Genomic DNA was isolated from cell pellets after proteinase K treatment. The ROS1 kinase domain was amplified by polymerase chain reaction (PCR) from the genomic DNA and sequenced bidirectionally using Sanger sequencing.

Cell culture conditions

Human embryonic kidney 293FT cells (Invitrogen) were cultured in Dulbecco's Modified Eagle Medium supplemented with 10% fetal bovine serum (FBS; D-10). Ba/F3 cells, which are immortalized murine bone marrow–derived pro-B cells, were cultured in D-10 media with or without 0.5 ng/mL of interleukin (IL)-3 (Invitrogen). Crizotinib-resistant ROS1 fusion–positive NSCLC patient-derived MGH047 cells were cultured in ACL-4 medium supplemented with 3% FBS (10).

Survival assays

To assess 72-hour drug treatment, 2,000 to 3,000 cells were plated in replicates of three to six in 96-well plates. Following drug treatments, the cells were incubated with the CellTiter-Glo Assay reagent (Promega) for 10 minutes. Luminescence was measured using a Centro LB 960 microplate luminometer (Berthold Technologies). The data were graphically displayed using GraphPad Prism version 5.0 (GraphPad Software). IC_{50} values were determined using a nonlinear regression model with a sigmoidal dose response in GraphPad.

Immunoblot analysis

Lysates were prepared as previously described (3, 12). Equal volumes of lysate were electrophoresed and immunoblotted with antibodies against phospho-ROS1 (Tyr2274), ROS1 (69D6), phospho-p42/44 ERK/MAPK (Thr202/Tyr204), p42/44 ERK/MAPK, phospho-Akt (Ser473; D9E), panAkt (C67E7), phospho-S6 ribosomal protein (Ser240/244, D68F8), S6 ribosomal protein (54D2), STAT3 (79D7), phospho-STAT3 (Tyr705; Cell Signaling Technology), GAPDH (6C5, Millipore), and β-actin (Sigma).

Retroviral infection

cDNA encoding WT or mutant CD74–ROS1 was cloned into 1,520 retroviral expression vectors (pLenti), and viruses were replicated in 293FT cells by transfecting with packaging plasmids. After retroviral infection, Ba/F3 cells were selected by incubation with puromycin (0.7 μg/mL) for 2 weeks. For Ba/F3 cells infected by CD74–ROS1 variants, IL3 was withdrawn from the culture medium at least 2 weeks before the experiments.

ENU mutagenesis screening

The ENU mutagenesis screening protocol was based on procedures published by Bradeen and colleagues (13) and O'Hare and colleagues (14). Briefly, ENU (Sigma) was dissolved in DMSO at a concentration of 100 mg/mL. All materials that came in contact with ENU were decontaminated with 0.2 mol/L NaOH. For each resistance screen, approximately 1.5×10^8 Ba/F3 CD74–ROS1 cells in a total of 160 mL of growth media were exposed to a final concentration of 100 μg/mL of ENU. After approximately 16 hours, the cells were collected by centrifugation, washed, and incubated for 24 hours. After a 24-hour recovery period, the cells were split into five aliquots of

Published OnlineFirst October 28, 2014; DOI: 10.1158/1078-0432.CCR-14-1385

3×10^7 cells each. Crizotinib or ceritinib was added at a final concentration of 30, 50, 100, or 200 nmol/L, and cells of each aliquot were distributed into five 96-well plates (5×10^4 cells in 200-μL media per well). Plates were incubated over a course of 4 weeks with regular inspection. When clear signs of cell growth were microscopically observed and a color change of the media occurred, the content of the respective well was transferred into 1 mL of growth media containing the original concentration of inhibitors in a 24-well plate. After approximately 1 week of expansion, the cell number was sufficient for further processing (see below).

Identification of ROS1 mutations

Genomic DNA was prepared by lysing the cells with proteinase K buffer, which was heat inactivated at 95°C for 5 minutes. Then, the temperature was gradually decreased by 2°C/min. For sequence analysis, a DNA fragment covering the entire kinase domain of ROS1 was amplified using KOD Plus (TOYOBO). The PCR products were then purified with a gel purification kit (GE healthcare) and sequenced using standard Sanger sequencing.

Drug screening

Inhibitor screening was conducted using a subset of the modified SCADS library containing 282 compounds in three 96-well microplates. Parental, CD74–ROS1 WT-, or CD74–ROS1–G2032R–expressing Ba/F3 cells were seeded in triplicates in 96-well plates on day 1, and each inhibitor was added at 10 nmol/L, 100 nmol/L, 1 μmol/L, and 3 μmol/L on the same day. Cell viability was determined on day 4 using the CellTiter-Glo Assay. The cell viability from triplicate plates was averaged to determine relative cell growth compared with that of DMSO-treated controls.

Statistical analysis

All data are presented as mean ± SD. Statistical analysis was performed using the two-tailed Student *t* test. Significance was established for P values < 0.05.

Results

Several ALK inhibitors effectively inhibit CD74–ROS1 fusion

The tyrosine kinase domains of ALK and ROS1 shared 70% identity, and both kinases belong to the same branch in a kinase phylogenic tree (11). To identify inhibitors capable of inhibiting the kinase activities of the ROS1 fusion protein, we tested the potency of various ALK inhibitors to CD74–ROS1. First, we established IL3 independently growing Ba/F3 cells by transformation with *CD74–ROS1*, which is the most frequently observed *ROS1* fusion gene in NSCLC. From the polyclonal CD74–ROS1–addicted Ba/F3 cells, we picked up the clone with a high expression of CD74–ROS1 and similar crizotinib sensitivity to the polyclonal cells (clone #6; Supplementary Fig. S1), which was propagated to examine the sensitivity to various ALK inhibitors currently being clinically evaluated. Our results showed that crizotinib, ceritinib (LDK378), and AP26113 exhibited remarkable growth suppression of CD74–ROS1 Ba/F3 cells, ASP3026 showed moderate inhibitory activity, and alectinib (CH5424802) showed none (Fig. 1A and B). Corresponding to the cell growth-inhibiting activity, crizotinib, ceritinib, AP26113, and ASP3026, but not alectinib, inhibited

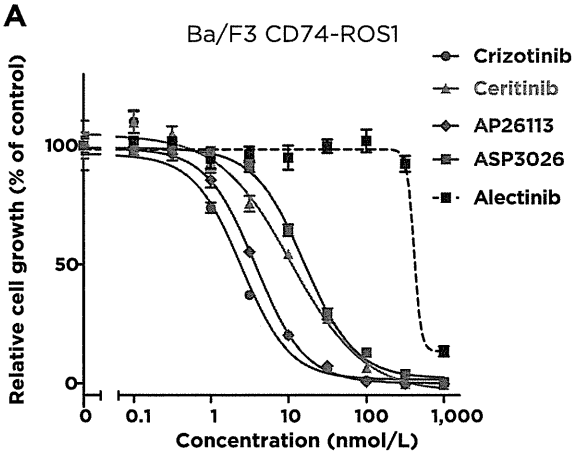

B

Drugs	IC_{50}(nmol/L)
Crizotinib	2.12
Ceritinib	10.92
AP26113	2.68
ASP3026	16.11
Alectinib	586.6

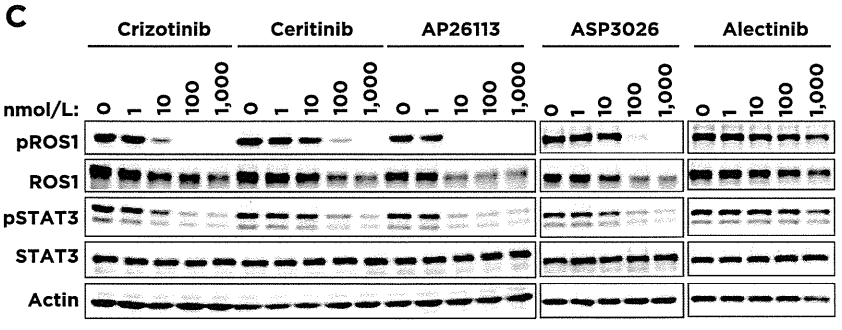

Figure 1.
Several ALK inhibitors effectively inhibit the growth of CD74–ROS1–addicted Ba/F3 cells. A, Ba/F3 cells expressing CD74–ROS1 (clone #6) were seeded in 96-well plates and treated with the indicated concentration of crizotinib, ceritinib, AP26113, ASP3026, or alectinib for 72 hours. Cell viability was analyzed using the CellTiter-Glo Assay. B, IC_{50} values (nmol/L) of Ba/F3 cell lines expressing CD74–ROS1 (clone #6) against various ALK inhibitors are shown. Average IC_{50} values against crizotinib, ceritinib, or AP26113 were calculated from the three independent experiments. IC_{50} values against ASP3026 and alectinib were calculated from the single experiment. C, inhibition of phospho-ROS1 by various ALK inhibitors in Ba/F3 models. CD74–ROS1–expressing Ba/F3 cells were exposed to increasing concentrations of crizotinib, ceritinib, AP26113, ASP3026, or alectinib for 3 hours. Cell lysates were immunoblotted to detect the indicated proteins.

Published OnlineFirst October 28, 2014; DOI: 10.1158/1078-0432.CCR-14-1385

phospho-ROS1 and its downstream phospho-STAT3 in a dose-dependent manner (Fig. 1C). Among these compounds, crizotinib and ceritinib are clinically available for ALK fusion–positive NSCLC. Furthermore, ceritinib, AP26113, and ASP3026 were shown to be active against the ALK gatekeeper mutation (L1196M), which is most frequently observed in crizotinib-resistant ALK-rearranged NSCLC (15). Therefore, we decided to identify potential resistance mechanisms to crizotinib or ceritinib in CD74–ROS1 mediated by a resistance mutation in the ROS1 kinase domain.

Identification of crizotinib- and ceritinib-resistant Ba/F3 CD74–ROS1 cells by accelerated mutagenesis screening

To identify *ROS1* mutations responsible for resistance to crizotinib or ceritinib in ROS1 fusion–positive cancers, we performed random mutagenesis screening by exposing the CD74–ROS1 Ba/F3 cells to the alkylating agent ENU, followed by selection using various concentration of crizotinib or ceritinib. After culturing with the inhibitors for 3 to 4 weeks, we observed an inhibitor dose-dependent reduction in the number of wells with growing cells. The resistant cells were recovered and the ROS1 kinase domains were sequenced. The resistant clones were selected by treatment with 200 nmol/L of crizotinib or ceritinib, and all carried the G2032R mutation (Fig. 2A). Of the clones selected with 100 nmol/L crizotinib, one clone harbored the K2003I mutation in the CD74–ROS1 and a second clone harbored no mutation. After expanding the isolated clone from ENU mutagenesis screening harboring K2003I mutated CD74–ROS1, we tested the sensitivity to crizotinib and ceritinib. We found that K2003I-mutated ROS1 did not confer resistance to crizotinib or ceritinib. On the other hand, G2032R-mutated CD74–ROS1 conferred high resistance to both crizotinib and ceritinib (Fig. 2B and C). When the cells were selected using a lower concentration of crizotinib (50 nmol/L) or ceritinib (100 nmol/L), various mutations in the clones were identified (Supplementary Fig. S2). Next, we tested the isolated clones from ENU mutagenesis for crizotinib or ceritinib sensitivity. The recovered Ba/F3 cells harboring the mutations E1990G with M2128V, L1951R, G2032R, or L2026M with K2003I in ROS1 showed IC_{50} values against crizotinib that were more than 3-fold higher than that of WT CD74–ROS1–expressing BaF3 cells (Supplementary Fig. S3A and S3B). On the other hand, Ba/F3 CD74–ROS1 cells harboring the L2026M mutation, which is a gatekeeper mutation corresponding to L1196M in ALK, were sensitive to ceritinib. Likewise, the mutations E1990G with M2128V, L1951R, or G2032R conferred resistance to ceritinib. In particular, the CD74–ROS1–expressing Ba/F3 cells harboring the G2032R mutation were extremely resistant to both crizotinib and ceritinib. Then, we conducted immunoblot analysis of the recovered Ba/F3 cells by treating the cells with various concentrations of crizotinib or ceritinib. The results were consistent with those of the cell viability assay, in which phosphorylation of CD74–ROS1 harboring the G2032R mutation was not completely attenuated even following treatment with 1 μmol/L of crizotinib or ceritinib (Fig. 2B). The G2032R mutation was recently identified in a patient with crizotinib refractory CD74–ROS1 fusion-positive NSCLC (10). In contrast, cells carrying the L1951R and E1990G with M2128V mutations exhibited resistance to crizotinib or ceritinib, consistent with the results of the cell viability assay. Cells harboring the L2026M/K2003I double mutant exhibited resistance to crizotinib but not to ceritinib (Supplementary Fig. S3C).

To confirm whether these mutations confer resistance to crizotinib and ceritinib, we introduced each mutated CD74–ROS1 in Ba/F3 cells. All of the resistant mutated CD74–ROS1 (L1951R, L1982F, E1990G, F1994L, K2003I, L2026M, and G2032R) maintained transforming activity. Then, we tested the sensitivity of Ba/F3 cells expressing CD74–ROS1 mutants to crizotinib or ceritinib. Similar to the result of the recovered Ba/F3 cells from ENU mutagenesis screening, L1951R and G2032R mutated CD74–ROS1–induced Ba/F3 cells showed marked

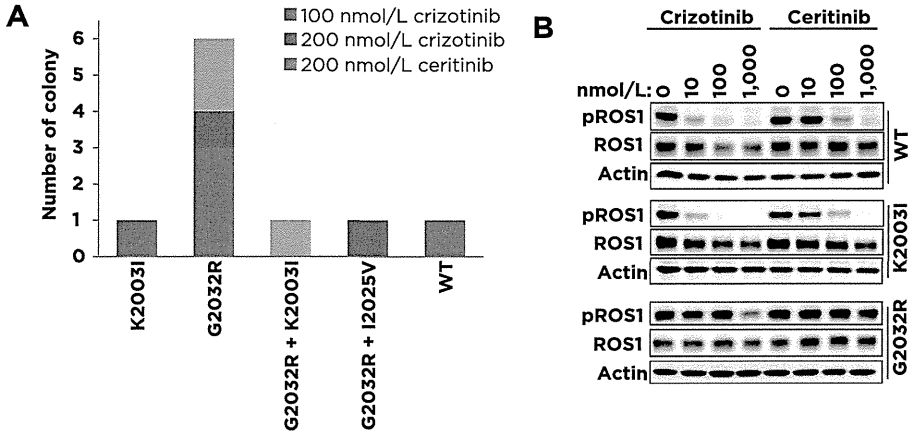

C

IC_{50} (nmol/L)	Crizotinib	Ceritinib
WT	2.12	10.92
K2003I	1.52	11.69
G2032R	253.7	276.5
Parental + IL3	370.0	1163

Figure 2.
Identification of crizotinib and ceritinib-resistant mutations by accelerated mutagenesis screening. A, number of the ROS1 kinase domain mutations found in the ENU-treated CD74–ROS1 Ba/F3 clones isolated after growth in the presence of 100 and 200 nmol/L of crizotinib or 200 nmol/L of ceritinib. B, inhibition of phospho-ROS1 by crizotinib and ceritinib in ENU-selected crizotinib- or ceritinib-resistant Ba/F3 clones. CD74–ROS1 WT–expressing Ba/F3 cell clone 6 or ENU-selected K2003I or Ba/F3 cells harboring the G2032R mutation were exposed to increasing concentrations of crizotinib or ceritinib for 2 hours. Cell lysates were immunoblotted to detect the indicated proteins. C, IC_{50} values for CD74–ROS1 kinase domain mutant Ba/F3 cells treated with crizotinib or ceritinib. IC_{50} values are shown in the lower table. IC_{50} values of Ba/F3 parental cells cultured with IL3 and CD74–ROS1 WT–expressing Ba/F3 cells are shown for comparison.

Published OnlineFirst October 28, 2014; DOI: 10.1158/1078-0432.CCR-14-1385

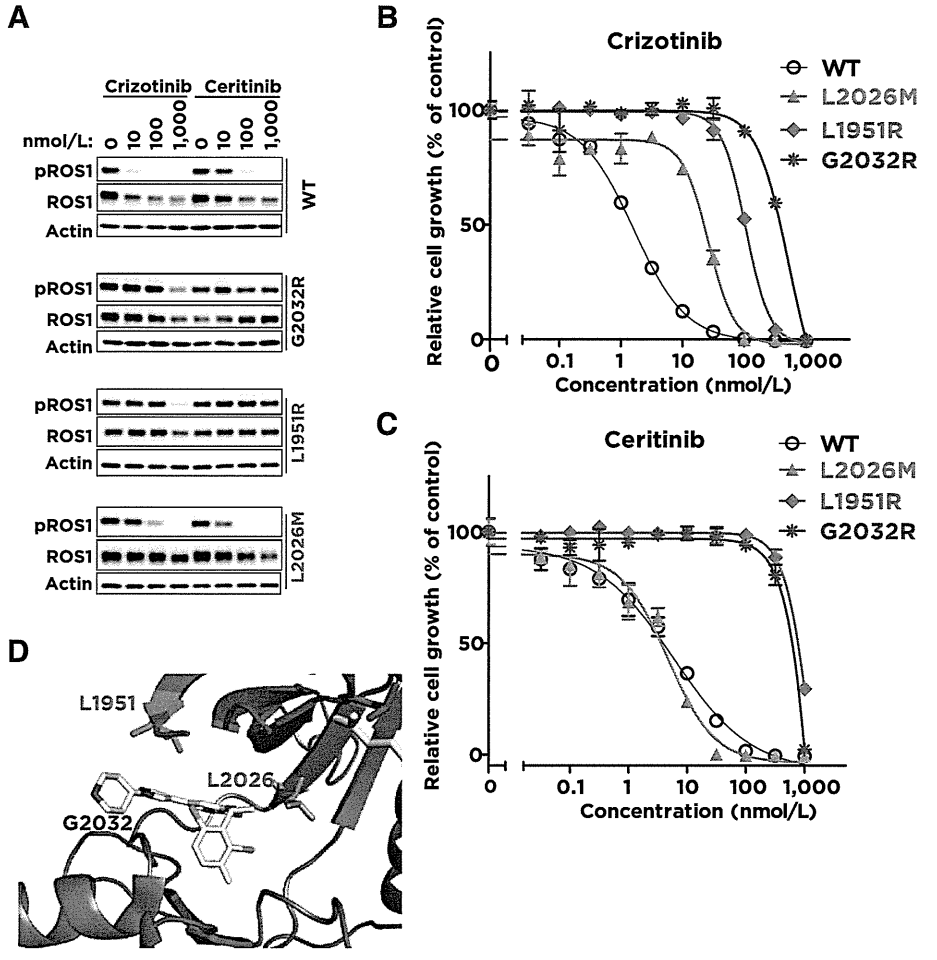

Figure 3.
Sensitivity of the CD74–ROS1 mutant-reintroduced Ba/F3 cells to crizotinib or ceritinib. A, inhibition of phospho-ROS1 by crizotinib and ceritinib in each WT or mutant CD74–ROS1–introduced Ba/F3 cell. Each Ba/F3 cell was exposed to increasing concentrations of crizotinib or ceritinib for 2 hours. Cell lysates were immunoblotted to detect the indicated proteins. B and C, WT or mutant (G2032R, L1951R, or L2026M) CD74–ROS1–introduced Ba/F3 cells were seeded on 96-well plates and treated with the indicated concentration of crizotinib (B) or ceritinib (C) for 72 hours. Cell viability was analyzed using the CellTiter-Glo Assay. IC_{50} values of each mutant Ba/F3 clone to crizotinib or ceritinib are shown in Supplementary Fig. S4A and B. D, resistant mutation residues in the structural models of WT ROS1 kinase domain with crizotinib. Three-dimensional mapping of each identified ROS1 mutation based on the crystal structure of ROS1 with crizotinib. Each of the three ROS1 mutations is mapped on a ribbon diagram. Figures were drawn using PyMol software with the crystal structure information of PDB ID 3ZBF. Other identified mutations mapped on the whole ROS1 kinase domain are shown in Supplementary Fig. S5.

resistance to crizotinib, ceritinib, and AP26113. L2026M mutant–induced Ba/F3 cells were resistant to crizotinib but not to ceritinib or AP26113. L1982F, E1990G, or F1994L mutants showed slight resistance to crizotinib and ceritinib. (Fig. 3A–C and Supplementary Fig. S4A–S4C).

Next, we mapped these mutations on the crystal structure data of crizotinib: ROS1 to elucidate the location of mutations that confer resistance (Fig. 3D and Supplementary Fig. S5). L1951 and G2032 mutations were located in the solvent-front region (entrance of the crizotinib-binding pocket), and L2026, which correspond to the L1196 mutation in ALK, is a gatekeeper mutation of ROS1. All of the identified mutations that conferred higher crizotinib resistance were located close to the crizotinib-binding domain of the ROS1 kinase (Fig. 3D).

High-throughput inhibitor screening identified cabozantinib (XL-184) as a potent ROS1 inhibitor

To identify potent ROS1 kinase inhibitors that selectively suppress the growth of Ba/F3 cells expressing either WT or the crizotinib-resistance mutant CD74–ROS1, we performed cell-based high-throughput screening with a series of kinase inhibitors and anticancer agents used in clinical practice or under current clinical evaluation. IL3-independent Ba/F3 cells expressing either WT or G2032R-mutated CD74–ROS1 were treated for 72 hours with serial dilutions of 282 kinase inhibitors and anticancer drugs in the SCAD inhibitor library. Potential ROS1 kinase inhibitors were selected for further evaluation using the following criteria: selective growth-inhibitory effect (<40% cell viability) against WT or G2032R-mutated Ba/F3 CD74–ROS1 cells at an inhibitor concentration of $\leq$100 nmol/L and $\geq$10-fold lower IC_{50} value compared with that for Ba/F3 parental cells. Using this assay, we newly demonstrated that cabozantinib (XL184), foretinib, TAE684, SB218078, and CEP701, in addition to the ALK inhibitors under clinical evaluation or in clinic, are potent inhibitors of CD74–ROS1 Ba/F3 cell growth (Table 1; Fig. 4A and B; Supplementary Table S1). Furthermore, among these inhibitors, cabozantinib (XL184), foretinib, and TAE684 effectively inhibited the growth of both WT and G2032R-mutated CD74–ROS1 Ba/F3 cells, and the autophosphorylation of both WT and CD74–ROS1 (Fig. 4B). Of note, CEP701 showed intermediate selectivity to the growth of CD74–ROS1 Ba/F3 cells, and CEP701 only inhibited the autophosphorylation of WT CD74–ROS1 but not the autophosphorylation of G2032R-mutated CD74–ROS1. And to inhibit the phospho-ROS1 of G2032R-mutated CD74–ROS1, higher concentration of TAE684, foretinib, or cabozantinib, compared with that for CD74–ROS1 (WT)–expressing Ba/F3 cells was needed (Fig. 4A and B).

Published OnlineFirst October 28, 2014; DOI: 10.1158/1078-0432.CCR-14-1385

Table 1. Kinase inhibitor screening identified multiple inhibitors active against CD74–ROS1 WT and G2032R crizotinib-resistant mutant

	Parental Ba/F3 (+IL3)				CD74–ROS1 WT				CD74–ROS1 (G2032R)			
	3 μmol/L	1 μmol/L	100 nmol/L	10 nmol/L	3 μmol/L	1 μmol/L	100 nmol/L	10 nmol/L	3 μmol/L	1 μmol/L	100 nmol/L	10 nmol/L
AP26113	**2.4**	**16.6**	101.6	104.7	**0.2**	**0.5**	**1.5**	**30.0**	**0.4**	**1.2**	76.5	114.8
Crizotinib	**2.5**	**5.2**	102.7	106.0	**1.4**	**1.9**	**4.4**	42.0	**2.7**	**2.3**	109.8	120.2
Ceritinib	**1.3**	74.8	104.6	103.0	**0.6**	**0.8**	**5.2**	62.1	**1.1**	**9.7**	102.2	109.3
ASP3026	69.4	96.3	110.7	100.9	**0.3**	**0.8**	**8.5**	74.9	**6.0**	58.8	101.0	110.0
SB218078	**4.1**	**5.9**	41.8	104.7	**1.3**	**1.9**	**1.9**	40.0	**2.2**	**3.1**	**28.9**	96.4
CEP701	**1.6**	**2.5**	47.3	96.6	**1.5**	**1.2**	**1.4**	**32.5**	**1.4**	**1.6**	**12.9**	97.0
TAE684	**1.6**	**8.9**	99.4	102.6	**0.3**	**0.5**	**0.9**	**10.7**	**0.5**	**0.5**	**10.1**	110.2
XL184	77.1	105.7	111.2	101.1	**0.3**	**1.0**	**1.1**	**21.2**	**0.5**	**0.6**	**5.6**	90.4
Foretinib	**3.3**	**2.8**	94.0	108.5	**0.5**	**0.7**	**1.7**	**32.3**	**0.7**	**0.7**	**14.9**	110.9

NOTE: The top 9 list of inhibitors, which specifically inhibit the growth of CD74–ROS1–expressing Ba/F3 cells, was obtained from high-throughput screening of 282 inhibitors. Ba/F3 parental cells (with IL3) or those expressing CD74–ROS1 WT or CD74–ROS1–G2032R were seeded in 96-well plates and treated with the indicated concentration of various inhibitors for 72 hours. Cell viability was analyzed using the CellTiter-Glo Assay. The average cell viability (% of control) of the top 9 inhibitors is shown. All of the screening data are shown in Supplementary Table S1.
Each number indicates cell viability (% of vehicle-treated control). Bold numbers indicate less than 40% of vehicle-treated control.

Cabozantinib overcomes the crizotinib-resistant CD74–ROS1 mutation

To examine the effect of cabozantinib on cells harboring these mutations, each of the Ba/F3 cells harboring the various CD74–ROS1 mutations (both ENU recovered Ba/F3 clones and CD74–ROS1 mutants–transformed Ba/F3 cells) were treated with cabozantinib, and the cell growth and phosphorylation of ROS1 were examined. The results showed that cabozantinib dose-dependently inhibited phospho-ROS1 in all crizotinib-resistant mutant strains and inhibited the growth of all Ba/F3 cells harboring crizotinib-resistant CD74–ROS1 mutations. IC_{50} values of all crizotinib-resistant mutants against cabozantinib were less than 25 nmol/L, although the IC_{50} values of crizotinib-resistant mutant (G2032R and L1951R) Ba/F3 cells were approximately 5- to 10-fold higher than that of WT CD74–ROS1 harboring Ba/F3 cells (Fig. 5 and Supplementary Figs. S6 and S7).

In our previous study of clinical crizotinib resistance in ROS1-rearranged NSCLC, we established the MGH047 cell line harboring the CD74–ROS1–G2032R mutation directly isolated from the pleural effusion of a crizotinib-resistant patient. Using this cell line, we compared the activities of cabozantinib and crizotinib and found that crizotinib did not inhibit the growth of MGH047 cells harboring the G2032R mutation, whereas cabozantinib potently inhibited the growth of MGH047 cells (Fig. 6A). Furthermore, as exhibited by the Ba/F3 cell line models, cabozantinib effectively suppressed phospho-ROS1 and downstream phospho-Akt, phospho-ERK, and phospho-ribosomal S6 proteins in MGH047 cells (Fig. 6B). These results suggest that cabozantinib presents an alternative therapeutic strategy to treat ROS1-rearranged NSCLC in both crizotinib-naïve patients and resistant cases caused by resistance mutations in the kinase domain.

Discussion

Recently, the cMET/ALK/ROS1 inhibitor crizotinib has been clinically evaluated for treatment of ROS1-rearranged NSCLC and has shown remarkable activity (8, 9). Because of the similarity between ROS1 and ALK kinase domains, we examined the sensitivity of various ALK inhibitors on CD74–ROS1 fusion and found that all the tested ALK inhibitors, except for alectinib, effectively inhibited ROS1 fusion. Among those ALK inhibitors, ceritinib was recently approved by the U.S. FDA for ALK-positive patients with crizotinib-resistant or crizotinib-intolerant disease, because high response rate in crizotinib-resistant disease was observed in phase I study (16). Ceritinib has also been shown to be active in both WT and gatekeeper-mutated ALK (L1196M), which causes crizotinib resistance (17). In *EGFR* mutant–positive lung cancers that become resistant to

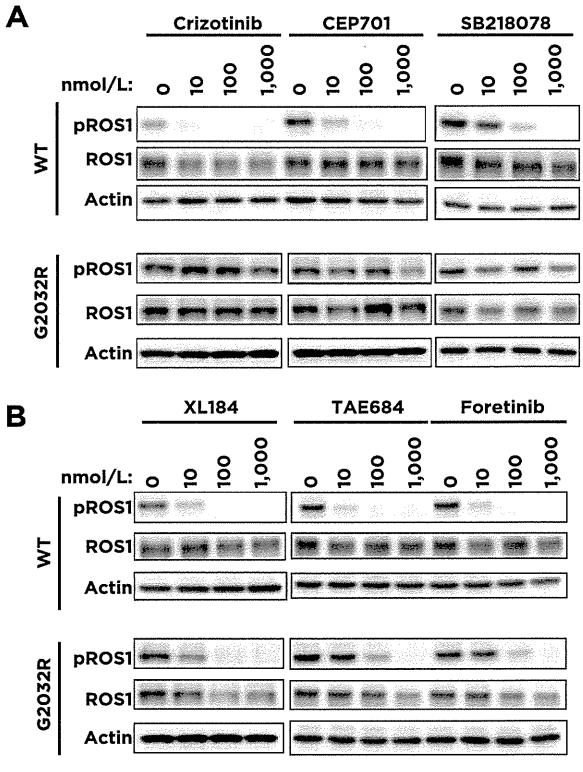

Figure 4.
Newly identified inhibitors effectively inhibit phospho-ROS1 of WT CD74–ROS1, or both WT and G2032R crizotinib-resistant mutant. A and B, inhibition of phospho-ROS1 by various identified ROS1 inhibitors selected from the high-throughput screening. CD74–ROS1 WT–expressing (clone 6) or CD74–ROS1–G2032R–expressing Ba/F3 cells were exposed to increasing concentrations of crizotinib, CEP701, SB218078 (A), cabozantinib (XL184), TAE684, or foretinib (B) for 2 hours. Following treatment, the cell lysates were immunoblotted to detect the indicated proteins.

Published OnlineFirst October 28, 2014; DOI: 10.1158/1078-0432.CCR-14-1385

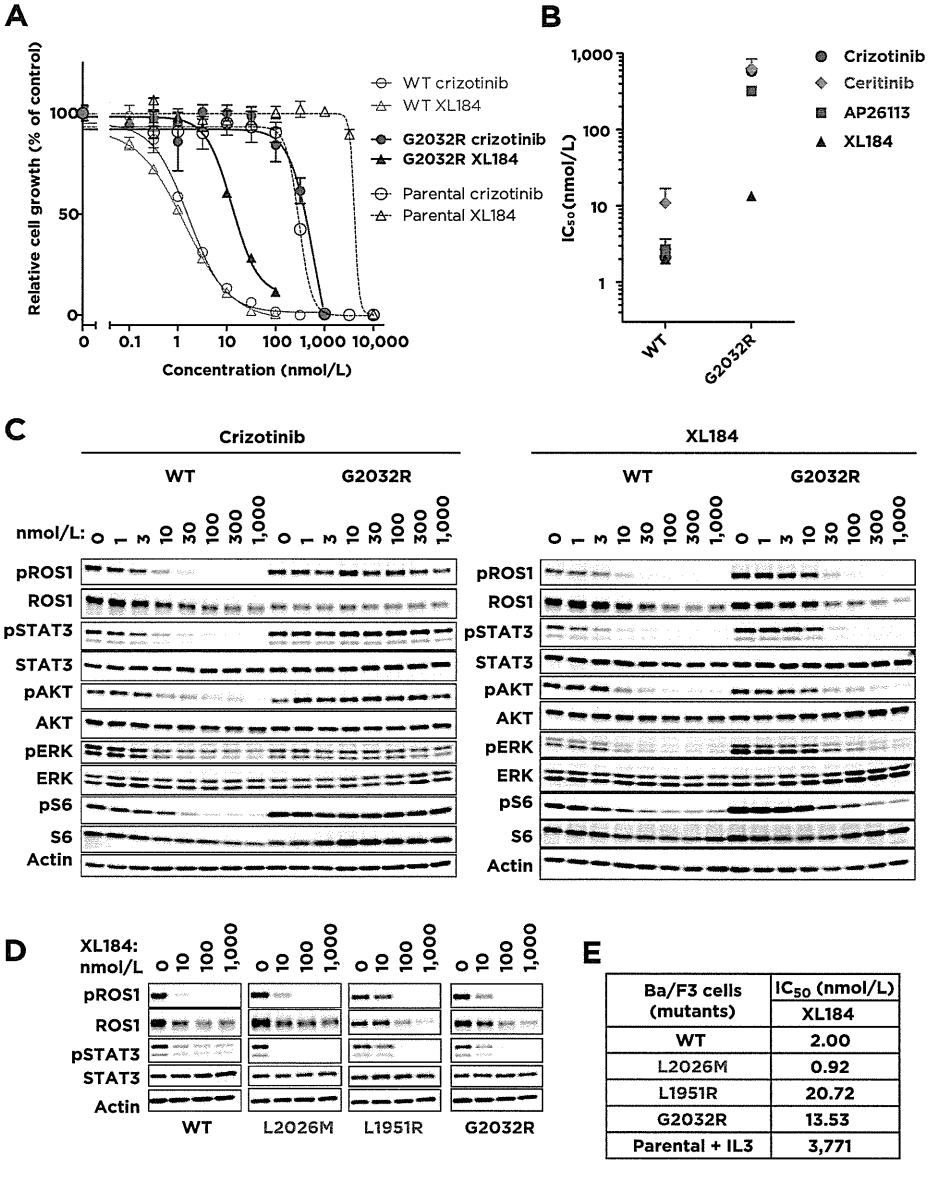

Figure 5.
Cabozantinib overcomes crizotinib resistance caused by the mutations in CD74–ROS1. A, Ba/F3 parental cells (with IL3) or those expressing CD74–ROS1 WT or CD74–ROS1–G2032R were seeded in 96-well plates and treated with the indicated concentration of crizotinib or cabozantinib (XL184) for 72 hours. Cell viability was analyzed using the CellTiter-Glo Assay. B, IC_{50} values of Ba/F3 cells expressing WT or G2032R-mutated CD74–ROS1 treated with crizotinib, ceritinib, AP26113, or cabozantinib (XL184). C, comparison of the inhibition of phospho-ROS1 and its downstream by crizotinib and cabozantinib in Ba/F3 cells expressing CD74–ROS1 WT or G2032R exposed to increasing concentrations of crizotinib or cabozantinib (XL-184) for 2 hours. Cell lysates were immunoblotted to detect the indicated proteins. D, inhibition of phospho-ROS1 by cabozantinib in each mutant expressing Ba/F3 cells. CD74–ROS1 WT or mutants expressing Ba/F3 cells were exposed to increasing concentrations of cabozantinib for 2 hours. Cell lysates were immunoblotted to detect the indicated proteins. E, average IC_{50} values (from the three independent experiments) of each Ba/F3 cells to cabozantinib (XL184) were shown.

E

Ba/F3 cells (mutants)	IC_{50} (nmol/L)
	XL184
WT	2.00
L2026M	0.92
L1951R	20.72
G2032R	13.53
Parental + IL3	3,771

EGFR TKIs, the secondary T790M gatekeeper mutation is detected in roughly one-half of all cases (2). In contrast, in crizotinib-resistant ALK-positive lung cancers, many types of resistance mutations in the ALK kinase domain were identified in various cell lines as well as crizotinib-resistant patients (3). Because the tyrosine kinase domains of ALK and ROS1 share approximately 70% homology, it is possible that many kinds of crizotinib-resistance mutations will also occur in ROS1-rearranged NSCLC.

To prospectively identify resistance mutations affecting the ALK/ROS1 inhibitors crizotinib and ceritinib, we performed a cellular drug resistance screen in CD74–ROS1–transformed Ba/F3 cells and identified several resistant mutations, including G2032R, as the most pronounced mutations that confer crizotinib resistance. So far, only the G2032R mutation in *ROS1* has been identified in crizotinib-treated resistant patients with *ROS1*-rearranged NSCLC (10). In this study, the newly identified resistance mutations of L1982F, E1990G, F1994L, and L2026M were less frequent and conveyed milder resistance to crizotinib. In addition, a screen with the structurally distinct ALK/ROS1 inhibitor ceritinib revealed a slightly different mutation profile; however, the most pronounced resistant mutations were L1951R and G2032R. In addition to ENU-induced accelerated mutagenesis screening, we also performed saturated mutagenesis screening (18–20) and identified different unique mutations (E2020K and P2021L), but no G2032R mutation was observed (data not shown). Similarly, a previous study using the same methods to identify crizotinib-resistance mutations in EML4–ALK identified unique mutations but did not recapitulate the clinically relevant mutations. These results suggest that induced mutation profiles in mismatch repair-deficient *Escherichia coli* strains might be slightly different from plausible

Published OnlineFirst October 28, 2014; DOI: 10.1158/1078-0432.CCR-14-1385

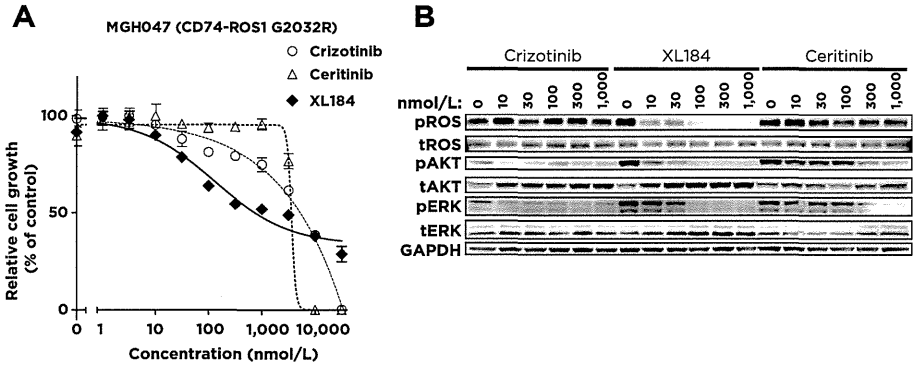

Figure 6.

Cabozantinib inhibits the growth of G2032R mutation harboring MGH047 cells and the phosphorylation of CD74–ROS1. A, crizotinib-resistant CD74–ROS1-positive NSCLC patient-derived MGH047 cells were seeded on 96-well plates and treated with the indicated concentration of crizotinib, ceritinib, or cabozantinib (XL184) for 7 days. Cell viability was analyzed using the CellTiter-Glo Assay. B, comparison of the inhibition of phospho-ROS1 and its downstream signaling by crizotinib, cabozantinib, or ceritinib in CD74–ROS1-G2032R-expressing MGH047 cells. MGH047 cells were exposed to the indicated concentrations of crizotinib, cabozantinib (XL184), or ceritinib for 6 hours. Cell lysates were immunoblotted to detect the indicated proteins.

mutations in mammalian cells. However, the mutagenesis screening study with imatinib in Ba/F3 cells harboring BCR–ABL fusion showed that the saturated screening assay is useful to identify various resistance mutations including those with clinical relevance (18).

The mutations identified from ENU-accelerated mutagenesis screening can be categorized into three types. The first type includes solvent-front mutations (e.g., L1951R and G2032R), which are located in the solvent-front region of the kinase domain adjacent to the crizotinib-binding site. An amino acid change of the conserved glycine to arginine at position 2032 or leucine to arginine at position 1951 of the ROS1 kinase domain confers considerable resistance to multiple ALK/ROS1 kinase inhibitors, such as crizotinib, ceritinib, and AP26113. The G2032R ROS1 mutation is analogous to the G1202R *ALK* mutation, which has been identified in *ALK*-rearranged lung cancers that have become resistant to crizotinib, alectinib, and ceritinib (3, 17). It is likely that these solvent-front mutations decrease the affinity of the mutant ROS1 for crizotinib because of steric hindrance (10).

The second type includes the gatekeeper mutation L2026M, which is equivalent to gatekeeper mutations observed in EGFR (T790M), ALK fusion (L1196M), and BCR–ABL (T315I). The third type is characterized by helix αC (L1982F or V), which is a homologous residue of L1152 in ALK, previously identified in patients with crizotinib-treated ALK-positive NSCLC (6).

To overcome resistance to crizotinib and ceritinib caused by the G2032R ROS1 mutation, we performed high-throughput drug screening, which subsequently identified cabozantinib (XL-184) as a potent ROS1 inhibitor that effectively inhibited both the WT CD74–ROS1 kinase as well as those harboring resistance mutations including G2032R. Furthermore, cabozantinib effectively inhibited the growth of the crizotinib-resistant patient-derived MGH047 cells harboring G2032R-mutated CD74–ROS1. Cabozantinib is a small molecule that inhibits the activity of multiple tyrosine kinases, including RET, MET, and VEGFR2. Currently, cabozantinib is clinically available for treatment of refractory medullary thyroid cancer. Data from previous clinical trials revealed a peak plasma concentration of cabozantinib after repeated oral administration (175 mg) of around 1,410 ng/mL (2810 nmol/L). Even in the much lower dose (0.64 mg/kg, which is corresponding to about 40-mg oral administration) treated patient, an average peak plasma concentration of cabozantinib after repeated oral administration was around 322 ng/mL (643 nmol/L; ref. 21). On the basis of the data from our study, we found that cabozantinib at concentrations less than 30 nmol/L inhibited all of the identified crizotinib-resistance mutations, which was much lower than clinically achievable levels. During the preparation of this manuscript, Davare and colleagues (22) identified that foretinib, which is an oral multikinase inhibitor targeting MET, VEGFR-2, RON, KIT, and AXL kinases and currently being clinically evaluated, is a potent inhibitor against ROS1 and overcomes resistance mutations including G2032R. Although we confirmed that foretinib also inhibited WT and all mutated crizotinib-resistance ROS1 fusions, our results suggest that cabozantinib is slightly more potent than foretinib. Furthermore, previously reported mean plasma concentrations of foretinib in two clinical trials were 72 and 340 nmol/L (23, 24). Although it is impossible to simply compare the plasma concentrations and expected efficacy in humans, cabozantinib is likely to be more potent and effective than foretinib.

In conclusion, our study clearly demonstrated that patients with crizotinib-resistant cancers due to an acquired mutation, such as G2032R, may benefit from more potent and effective ROS1 TKI. Notably, although solvent-front mutations are occasionally observed in patients with crizotinib-resistant ALK fusion-positive NSCLC, the frequency of G2032R mutations in ROS1-positive NSCLC has yet to be established. Because secondary mutations, such as the gatekeeper mutation, may not represent the predominant mechanism of acquired crizotinib resistance, additional studies are needed to elucidate other mechanisms of resistance. The results of these studies will be critical to selecting the best therapeutic strategies for targeting TKI resistance in clinical practice. Although, crizotinib is currently a key agent used to treat cancers harboring *ROS1* translocations, cabozantinib may be able to prevent or overcome resistance to ROS1 inhibitors.

Published OnlineFirst October 28, 2014; DOI: 10.1158/1078-0432.CCR-14-1385

Disclosure of Potential Conflicts of Interest

A.T. Shaw is a consultant/advisory board member for Genentech, Ignyta, Novartis, and Pfizer. J.A. Engelman reports receiving a commercial research grant from AstraZeneca, Novartis, and Sanofi-Aventis, and is a consultant/advisory board member for Novartis and Sanofi-Aventis. No potential conflicts of interest were disclosed by the other authors.

Authors' Contributions

Conception and design: R. Katayama, J.A. Engelman, N. Fujita
Development of methodology: R. Katayama, Y. Kobayashi
Acquisition of data (provided animals, acquired and managed patients, provided facilities, etc.): R. Katayama, Y. Kobayashi, L. Friboulet, E.L. Lockerman, S. Koike, A.T. Shaw
Analysis and interpretation of data (e.g., statistical analysis, biostatistics, computational analysis): R. Katayama, Y. Kobayashi, S. Koike
Writing, review, and/or revision of the manuscript: R. Katayama, A.T. Shaw, J.A. Engelman, N. Fujita
Administrative, technical, or material support (i.e., reporting or organizing data, constructing databases): Y. Kobayashi, S. Koike, N. Fujita
Study supervision: R. Katayama, J.A. Engelman, N. Fujita

Acknowledgments

The authors thank Dr. Mark M. Awad at Massachusetts General Hospital (MGH; Boston, MA) for helping with the establishment of MGH047 cells and Ms. Sidra Mahmood at MGH for helping with the cell survival assay experiments of MGH047 cells.

Grant Support

The study was supported, in part, by Japan Society for the Promotion of Science (JSPS) KAKENHI grant numbers 24300344 and 22112008 (to N. Fujita) and 25710015 (to R. Katayama), by NIH grant R01CA164273 (to A.T. Shaw and J.A. Engelman), and by a research grant from the Princess Takamatsu Cancer Research Fund (to N. Fujita).

The costs of publication of this article were defrayed in part by the payment of page charges. This article must therefore be hereby marked *advertisement* in accordance with 18 U.S.C. Section 1734 solely to indicate this fact.

Received May 29, 2014; revised August 19, 2014; accepted October 1, 2014; published OnlineFirst October 28, 2014.

References

1. Takeuchi K, Soda M, Togashi Y, Suzuki R, Sakata S, Hatano S, et al. RET, ROS1 and ALK fusions in lung cancer. Nat Med 2012;18:378–81.
2. Sequist LV, Waltman BA, Dias-Santagata D, Digumarthy S, Turke AB, Fidias P, et al. Genotypic and histological evolution of lung cancers acquiring resistance to EGFR inhibitors. Sci Transl Med 2011;3:75ra26.
3. Katayama R, Shaw AT, Khan TM, Mino-Kenudson M, Solomon BJ, Halmos B, et al. Mechanisms of acquired crizotinib resistance in ALK-rearranged lung Cancers. Sci Transl Med 2012;4:120ra17.
4. Choi YL, Soda M, Yamashita Y, Ueno T, Takashima J, Nakajima T, et al. EML4-ALK mutations in lung cancer that confer resistance to ALK inhibitors. N Engl J Med 2010;363:1734–9.
5. Doebele RC, Pilling AB, Aisner DL, Kutateladze TG, Le AT, Weickhardt AJ, et al. Mechanisms of resistance to crizotinib in patients with ALK gene rearranged non–small cell lung cancer. Clin Cancer Res 2012;18:1472–82.
6. Sasaki T, Koivunen J, Ogino A, Yanagita M, Nikiforow S, Zheng W, et al. A novel ALK secondary mutation and EGFR signaling cause resistance to ALK kinase inhibitors. Cancer Res 2011;71:6051–60.
7. Sasaki T, Okuda K, Zheng W, Butrynski J, Capelletti M, Wang L, et al. The neuroblastoma associated F1174L ALK mutation causes resistance to an ALK kinase inhibitor in ALK translocated cancers. Cancer Res 2010;70:10038–43.
8. Bergethon K, Shaw AT, Ou SH, Katayama R, Lovly CM, McDonald NT, et al. ROS1 rearrangements define a unique molecular class of lung cancers. J Clin Oncol 2012;30:863–70.
9. Shaw AT, Camidge DR, Engelman JA. Clinical activity of crizotinib in advanced non–small cell lung cancer (NSCLC) harboring ROS1 gene rearrangement. J Clin Oncol 30, 2012 (suppl; abstr 7508).
10. Awad MM, Katayama R, McTigue M, Liu W, Deng YL, Brooun A, et al. Acquired resistance to crizotinib from a mutation in CD74–ROS1. N Engl J Med 2013;368:2395–401.
11. Manning G, Whyte DB, Martinez R, Hunter T, Sudarsanam S. The protein kinase complement of the human genome. Science 2002;298:1912–34.
12. Engelman JA, Zejnullahu K, Mitsudomi T, Song Y, Hyland C, Park JO, et al. MET amplification leads to gefitinib resistance in lung cancer by activating ERBB3 signaling. Science 2007;316:1039–43.
13. Bradeen HA, Eide CA, O'Hare T, Johnson KJ, Willis SG, Lee FY, et al. Comparison of imatinib mesylate, dasatinib (BMS-354825), and nilotinib (AMN107) in an N-ethyl-N-nitrosourea (ENU)-based mutagenesis screen: high efficacy of drug combinations. Blood 2006;108:2332–8.
14. O'Hare T, Eide CA, Tyner JW, Corbin AS, Wong MJ, Buchanan S, et al. SGX393 inhibits the CML mutant Bcr-AblT315I and preempts *in vitro* resistance when combined with nilotinib or dasatinib. Proc Natl Acad Sci U S A 2008;105:5507–12.
15. Lovly CM, Pao W. Escaping ALK inhibition: mechanisms of and strategies to overcome resistance. Sci Transl Med 2012;4:120ps2.
16. Shaw AT, Kim DW, Mehra R, Tan DS, Felip E, Chow LQ, et al. Ceritinib in ALK-rearranged non–small-cell lung cancer. N Engl J Med 2014;370:1189–97.
17. Friboulet L, Li N, Katayama R, Lee CC, Gainor JF, Crystal AS, et al. The ALK inhibitor ceritinib overcomes crizotinib resistance in non–small cell lung cancer. Cancer Discov 2014;4:662–73.
18. Azam M, Latek RR, Daley GQ. Mechanisms of autoinhibition and STI-571/imatinib resistance revealed by mutagenesis of BCR–ABL. Cell 2003;112:831–43.
19. Emery CM, Vijayendran KG, Zipser MC, Sawyer AM, Niu L, Kim JJ, et al. MEK1 mutations confer resistance to MEK and B-RAF inhibition. Proc Natl Acad Sci U S A 2009;106:20411–6.
20. Heuckmann JM, Holzel M, Sos ML, Heynck S, Balke-Want H, Koker M, et al. ALK mutations conferring differential resistance to structurally diverse ALK inhibitors. Clin Cancer Res 2011;17:7394–401.
21. Kurzrock R, Sherman SI, Ball DW, Forastiere AA, Cohen RB, Mehra R, et al. Activity of XL184 (Cabozantinib), an oral tyrosine kinase inhibitor, in patients with medullary thyroid cancer. J Clin Oncol 2011;29:2660–6.
22. Davare MA, Saborowski A, Eide CA, Tognon C, Smith RL, Elferich J, et al. Foretinib is a potent inhibitor of oncogenic ROS1 fusion proteins. Proc Natl Acad Sci U S A 2013;110:19519–24.
23. Eder JP, Shapiro GI, Appleman LJ, Zhu AX, Miles D, Keer H, et al. A phase I study of foretinib, a multi-targeted inhibitor of c-Met and vascular endothelial growth factor receptor 2. Clin Cancer Res 2010;16:3507–16.
24. Shapiro GI, McCallum S, Adams LM, Sherman L, Weller S, Swann S, et al. A Phase 1 dose-escalation study of the safety and pharmacokinetics of once-daily oral foretinib, a multi-kinase inhibitor, in patients with solid tumors. Invest New Drugs 2013;31:742–50.

Published OnlineFirst October 13, 2014; DOI: 10.1158/1535-7163.MCT-14-0462

Small Molecule Therapeutics

Molecular Cancer Therapeutics

Tivantinib (ARQ 197) Exhibits Antitumor Activity by Directly Interacting with Tubulin and Overcomes ABC Transporter–Mediated Drug Resistance

Aki Aoyama[1,2], Ryohei Katayama[1], Tomoko Oh-hara[1], Shigeo Sato[1], Yasushi Okuno[3], and Naoya Fujita[1,2]

Abstract

Tivantinib (ARQ197) was first reported as a highly selective inhibitor of c-MET and is currently being investigated in a phase III clinical trial. However, as recently reported by us and another group, tivantinib showed cytotoxic activity independent of cellular c-MET status and also disrupted microtubule dynamics. To investigate if tivantinib exerts its cytotoxic activity by disrupting microtubules, we quantified polymerized tubulin in cells and xenograft tumors after tivantinib treatment. Consistent with our previous report, tivantinib reduced tubulin polymerization in cells and in mouse xenograft tumors *in vivo*. To determine if tivantinib directly binds to tubulin, we performed an *in vitro* competition assay. Tivantinib competitively inhibited colchicine but not vincristine or vinblastine binding to purified tubulin. These results imply that tivantinib directly binds to the colchicine binding site of tubulin. To predict the binding mode of tivantinib with tubulin, we performed computer simulation of the docking pose of tivantinib with tubulin using GOLD docking program. Computer simulation predicts tivantinib fitted into the colchicine binding pocket of tubulin without steric hindrance. Furthermore, tivantinib showed similar IC_{50} values against parental and multidrug-resistant cells. In contrast, other microtubule-targeting drugs, such as vincristine, paclitaxel, and colchicine, could not suppress the growth of cells overexpressing ABC transporters. Moreover, the expression level of ABC transporters did not correlate with the apoptosis-inducing ability of tivantinib different from other microtubule inhibitor. These results suggest that tivantinib can overcome ABC transporter–mediated multidrug-resistant tumor cells and is potentially useful against various tumors. *Mol Cancer Ther; 13(12); 2978–90. ©2014 AACR.*

Introduction

The receptor tyrosine kinase, *MET* proto-oncogene, receptor tyrosine kinase (c-MET) is a high-affinity receptor for hepatocyte growth factor (HGF), and its downstream v-*akt* murine thymoma viral oncogene homolog 1 (AKT) and mitogen-activated protein kinase 1 (ERK) pathways are regulated by HGF/c-MET. The HGF/c-MET axis is involved in cancer progression, metastasis, and acquired resistance. HGF/c-MET signaling is often highly activated in tumors because of various mechanisms (1). Because c-MET–addicted cancers have been shown to be highly sensitive to c-MET kinase inhibitors *in vitro* and *in vivo*, c-MET is recognized as a therapeutic target, and some c-MET inhibitors are currently being evaluated in clinical trials (2).

Tivantinib (ARQ197) was first reported to be a highly selective inhibitor of c-MET (3). Crystal structure analysis elucidated a unique mechanism in which tivantinib preferentially binds to the inactive form of c-MET. In addition, unlike other c-MET inhibitors, tivantinib inhibits c-MET through a non–ATP-competitive mechanism (4). From the results of a phase I clinical trial, tivantinib showed encouraging antitumor activity and tolerability (5). In early clinical trials, tivantinib increased overall survival (OS) and progression-free survival (PFS) in patients with hepatocellular cancer showing high c-MET expression. On the basis of these data, the phase III trial currently ongoing enrolls only MET-high patients (6). On the other hand, in a recent clinical trial of tivantinib combined with an epidermal growth factor receptor (EGFR) tyrosine kinase inhibitor (TKI), there were no significant differences in PFS and OS between the study arm (tivantinib with EGFR-TKI) and control arm (EGFR-TKI only; ref. 7). Surprisingly, subgroup analysis showed that tivantinib with EGFR-TKI treatment significantly improved PFS among patients with non–small cell lung cancer (NSCLC) with Kirsten rat sarcoma viral oncogene homolog (*KRAS*) mutation, but the latest phase III data presented at European Cancer

[1]The Cancer Chemotherapy Center, Japanese Foundation for Cancer Research, Tokyo, Japan. [2]Department of Medical Genome Sciences, Graduate School of Frontier Sciences, The University of Tokyo, Tokyo, Japan. [3]Graduate School of Medicine, Kyoto University, Kyoto, Japan.

Note: Supplementary data for this article are available at Molecular Cancer Therapeutics Online (http://mct.aacrjournals.org/).

A. Aoyama and R. Katayama contributed equally to this article.

Corresponding Author: Naoya Fujita, Japanese Foundation for Cancer Research, 3-8-31, Ariake, Koto-ku, Tokyo, 135-8550, Japan. Phone: 81-3-3570-0468; Fax: 81-3-3570-0484; E-mail: naoya.fujita@jfcr.or.jp

doi: 10.1158/1535-7163.MCT-14-0462